2004

Needle-based ablation of renal parenchyma using microwave, cryoablation, impedance- and temperature-based monopolar and bipolar radiofrequency, and liquid and gel chemoablation: Laboratory studies and review of the literature

Jamil Rehman
SUNY Stony Brook

Jaime Landman
Washington University School of Medicine in St. Louis

David Lee
University of California - Irvine

Ramakrishna Venkatesh
Washington University School of Medicine in St. Louis

David G. Bostwick
Bostwick Laboratories

JOURNAL OF ENDOUROLOGY
Volume 18, Number 1, February 2004

Needle-Based Ablation of Renal Parenchyma Using Microwave, Cryoablation, Impedance- and Temperature-Based Monopolar and Bipolar Radiofrequency, and Liquid and Gel Chemoablation: Laboratory Studies and Review of the Literature

JAMIL REHMAN, M.D.,[1] JAIME LANDMAN, M.D.,[2] DAVID LEE, M.D.,[3] RAMAKRISHNA VENKATESH, M.D.,[2] DAVID G. BOSTWICK, M.D.,[4] CHANDRU SUNDARAM, M.D.,[5] and RALPH V. CLAYMAN, M.D.[3]

ABSTRACT

***Background and Purpose*: Small renal tumors are often serendipitously detected during the screening of patients for renal or other disease entities. Rather than perform a radical or partial nephrectomy for these diminutive lesions, several centers have begun to explore a variety of ablative energy sources that could be applied directly via a percutaneously placed needle-like probe. To evaluate the utility of such treatment for small renal tumors/masses, we compared the feasibility, regularity (consistency in size and shape), and reproducibility of necrosis produced in normal porcine kidneys by different modes of tissue ablation: microwaves, cold impedance-based and temperature-based radiofrequency (RF) energy (monopolar and bipolar), and chemical. Chemoablation was accomplished using ethanol gel, hypertonic saline gel, and acetic acid gel either alone or with simultaneous application of monopolar or bipolar RF energy.**

***Materials and Methods*: A total of 107 renal lesions were created laparoscopically in 33 domestic pigs. Microwave thermoablation (N = 12) was done using a Targis T3 (Urologix) 10F antenna. Cryoablation (N = 16) was done using a single 1.5-mm probe or three 17F microprobes (17F SeedNet™ system; Galil Medical) (N = 10 single probe and N = 6 three probes); a double freeze cycle with a passive thaw was employed under ultrasound guidance. Dry RF lesions were created using custom-made 18-gauge single-needle monopolar probe with two or three exposed metal tips (GelTx) (N = 12) or a single-needle bipolar probe (N = 6) at 50 W of 510 kHz RF energy for 5 minutes. In addition, a multitine RF probe (RITA Medical Systems) was used in one set of studies (N = 6). Both impedance- and temperature-based RF were evaluated. Chemoablation was performed with 95% ethanol (4 mL), 24% hypertonic saline (4 mL), and 50% acetic acid (4 mL) as single injections. In addition, chemoablation was tested with monopolar and bipolar RF (wet RF). Tissues were harvested 1 week after ablation for light microscopy.**

***Results*: In 11 of the 15 ablation techniques, there was complete necrosis in all lesions; however, three ethanol gel lesions had skip areas, three hypertonic saline gel lesions showed no necrosis or injury, and one monopolar RF and one bipolar RF lesion showed skip areas. In contrast to impedance-based RF, heat-based RF (RITA) caused complete necrosis without skip areas. All cryolesions resulted in complete tissue necrosis, and cryotherapy was the only modality for which lesion size could be effectively monitored using ultrasound imaging.**

[1]Department of Urology, School of Medicine, SUNY-Stony Brook University, Stony Brook, New York.
[2]Department of Surgery, Division of Urologic Surgery, Washington University School of Medicine, St. Louis, Missouri.
[3]Department of Urology, School of Medicine, University of California, Irvine, California.
[4]Bostwick Laboratories, Richmond, Virginia.
[5]Department of Urology, Indiana University School of Medicine, Indianapolis, Indiana.

***Conclusions*: Cryoablation and thermotherapy produce well-delineated, completely necrotic renal lesions. The single-probe monopolar and bipolar RF produce limited areas of tissue necrosis; however, both are enhanced by using hypertonic saline, acetic acid, or ethanol gel. Hypertonic saline gel with RF consistently provided the largest lesions. Ethanol and hypertonic saline gels tested alone failed to produce consistent cellular necrosis at 1 week. In contrast, RITA using the Starburst™ XL probe produced consistent necrosis, while impedance-based RF left skip areas of viable tissue. Renal cryotherapy under ultrasound surveillance produced hypoechoic lesions, which could be reasonably monitored, while all other modalities yielded hyperechoic lesions the margins of which could not be properly monitored with ultrasound imaging.**

INTRODUCTION

WIDESPREAD APPLICATION OF CT and abdominal ultrasonography has led to an increase in the detection of small localized solid renal masses.[1–4] These renal masses are associated with a significant clinical dilemma, as 20% to 30% are benign. Unfortunately, percutaneous biopsy of these small lesions is unreliable. Indeed, Zincke and associates, who prospectively analyzed 106 intraoperative renal biopsies, found the overall accuracy to be only 76% to 80%, with 22% of the lesions being benign.[5]

Accordingly, except in the elderly or extremely high-risk patient, excisional surgery is usually selected. Traditionally, these patients have been treated with radical nephrectomy [1,2,6] or, more recently, nephron-sparing surgery.[1,7–15] However, in agreement with Bell's original work more than 70 years ago, a recent series by Walther and colleagues showed that no tumor <3 cm was associated with metastasis.[16] For these small lesions, the current literature suggests that with partial nephrectomy, crude and cause-specific survival is comparable to those obtained with radical nephrectomy for small (≤ 4 cm), low-grade, low-stage renal-cell carcinoma out to 10 years.[17] Concerns over satellite lesions are certainly valid for larger tumors; however, the incidence of satellite malignant lesions when the primary lesion is ≤ 3 cm is only 3.7%.[18]

In an effort to decrease the morbidity of open nephron-sparing surgery, laparoscopic partial nephrectomy and wedge excision of small renal masses have been reported; however, these techniques are still in their earliest stages. Moreover, they are often lengthy and require a high degree of skill on the part of the laparoscopic surgeon. In contrast, recent reports of laparoscopic needle ablative surgery, using predominantly cryotherapy or, less commonly, radiofrequency (RF) energy, have been shown to result in a less complex, yet apparently effective, ablative procedure. Even less invasive than the laparoscopic approach are needle-based therapies using MR or CT guidance for needle placement and treatment monitoring. The advantages of percutaneous needle ablation include minimal morbidity, low cost, suitability for real-time imaging guidance, and the appropriateness for performance in an outpatient setting.

To evaluate the effectiveness of needle ablative therapy in the kidney, we compared the regularity and reproducibility of necrosis produced in normal porcine kidneys by several energy sources: microwave thermotherapy (MT), cryotherapy, monopolar and bipolar single-needle RF using both impedance- and temperature-controlled monitoring, multitine monopolar RF, and monopolar and bipolar RF combined with ethanol, acetic acid, or hypertonic saline gel infusion. In addition, each of the three gels was tested as an ablative therapy in its own right.

MATERIALS AND METHODS

General approach

Laparoscopic procedure: A series of 33 female domestic pigs (50–70 kg) were used. After being anesthetized, the pigs were placed in a 30° Trendelenburg supine position, and pneumoperitoneum was achieved with a Veress needle via an infraumbilical puncture. A 12-mm laparoscopic port was placed via this incision, and a 10-mm laparoscope was inserted. The pig was rearranged in the lateral decubitus position, and under direct vision, two more 12-mm trocars were inserted in the midaxillary line above and below the level of the umbilicus. The upper and lower poles of the kidney were dissected. Just prior to the delivery of any needle-based ablative energy, surgical sponges were placed around the kidney to help prevent damage to adjacent visceral structures. The sponges were inserted and removed through a 12-mm port.

Tissue harvesting and histopathologic examination: The animals were sacrificed 1 week after ablative therapy, and their kidneys were harvested. This time frame was selected to permit analysis of the destructive effects of each modality at the cellular level. The abdominal cavity was explored to rule out any damage to other organs and to identify any adhesions. Both kidneys were removed for anatomic and histologic evaluation. Gross measurements of the field of ablation were made in three dimensions (length, width, and depth) using calipers after each kidney had been bivalved through the center of the treated field. All sections were fixed in 10% Formalin, sectioned, and embedded in paraffin. Hematoxylin and eosin (H&E) staining was performed. The size of the lesion, completeness of ablation, evidence of complications, and viability of the remainder of the kidney were assessed. Histopathologic analysis was performed by a skilled genitourinary tract pathologist (DJB).

Cryotherapy

Animals: Seven pigs were used in this study.

Cryosurgical system and temperature monitoring: Cryoprobes were from the 17-gauge SeedNet™ system (Galil Medical, Yokneam, Israel); the needles were constructed to be used with argon gas (Fig. 1). This system consisted of a computer workstation, a gas gauge, a gas distribution system, and accessories including needle-like cryoprobes, temperature sensors, and a remote control device. It used high-pressure cooling gas (argon), which achieved temperatures as low as -185°C at the tip of the needle probes.[19] To thaw the tissues rapidly, a high-pressure gas (helium) was converted to a warm low-pressure gas. Each cryoprobe was equipped with a thermocouple that monitored needle-tip temperature throughout freezing and thawing. A computer interface dis-

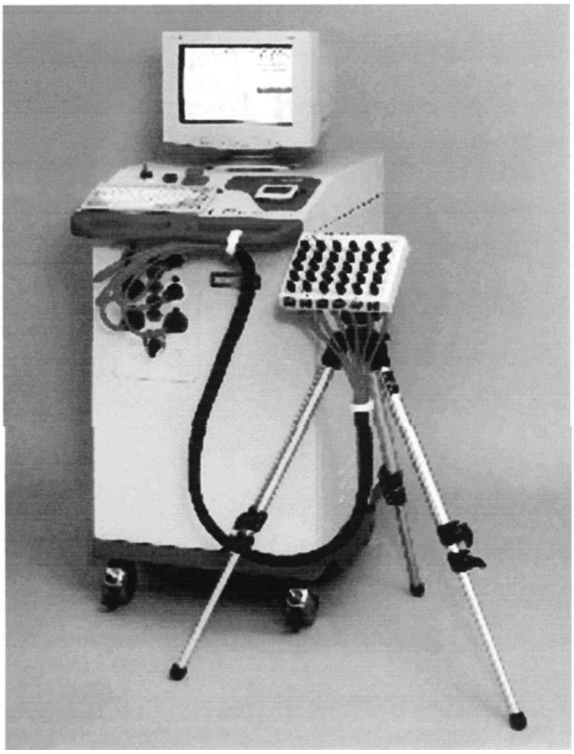

FIG. 1. Cryotherapy system (Galil™) uses 17 F cryotherapy needle probes (SeedNet™).

played needle-tip temperatures and was used to specify the desired temperature during the procedure. Heat exchange occurred only along a 4-cm segment at the distal end of each cryoprobe. Three cryoprobes can be used simultaneously in one or more locations and frozen or thawed independently. Separate trials were done with both a single- and a three-probe array.

Delivery of cryotherapy: The needles were inserted from anterior (ventral) to posterior (dorsal) under transperitoneal laparoscopic and ultrasound guidance (Tetrad US system). All probes were inserted to a depth of 7 to 8 mm to avoid entering the collecting system. The needle tips are echogenic, allowing their placement to be monitored by ultrasonography. The progress of the cryoablation was easily monitored by observing the advance of the iceball's hyperechoic rim. Cryoprobes were placed through the skin or a laparoscopic port. Thermosensors were also inserted into the renal parenchyma at 3-mm intervals (six sites per kidney) so that data would be collected both within and beyond the iceball. When a three-probe array was used, the needles were placed sufficiently close to one another to allow the iceballs to overlap. Freezing was measured continuously. Two freeze-thaw cycles (15-minute freeze, 10-minute passive thaw) were used. During freezing, the cryoprobe tip temperatures reached a nadir of −140° to −160°C. After the second freeze, the probes were retracted. Overall, 16 lesions were created, 10 with a single probe and 6 with the three-probe array.

Microwave thermotherapy

Animals: Three pigs were used.

Microwave thermotherapy control unit and heating antenna (end-fed gamma-matched helical dipole antenna): A modified MT system (Targis T3; Urologix, Minneapolis, MN) was utilized to deliver controlled microwave energy via a microwave antenna (Fig. 2). The system generator output has a maximum of 60 W at 1296 MHz. The control unit fiberoptic, as well as a resistive thermal device, "RTD," was used to monitor intralesional temperatures as well as the temperature around the antenna in real time. For this particular experiment, power was adjusted to achieve between 80° and 95°C adjacent to the antenna, which typically required 10 to 20 W. The device we used was a 10F, 2-cm long bare antenna. The treatment duration was 15 minutes. Twelve kidney lesions were created (two lesions per kidney in both the upper and the lower poles).

Placement of heating antenna and creation of lesion: The antenna was placed in the kidney parenchyma under ultrasound guidance, being careful to avoid entry into the collecting system.

Radiofrequency energy using single-needle monopolar and bipolar electrode probes

Animals: Five pigs were used.

Radiofrequency system and temperature-monitoring equipment and technique: An RF generator (Valleylab IIC electrosurgical generator) with an output of 50 W at 500 kHz was used. Separate laparoscopic needle electrodes (18-gauge, 2 cm of exposed metal distal tip [Prosurg/Injectx, San Jose, CA]) were used for monopolar and bipolar RF (Fig. 3). Grounding for the monopolar trials was achieved by attaching a dispersive pad to the pig's buttock (surface area >400 cm^2). The needle electrode was then connected to the RF generator. In the bipolar electrode, the active and receiving portions were spaced 1 cm apart on the shaft of the needle. These RF needle were impedance based for their regulation.

FIG. 2. Urologix T3 microwave system with antenna.

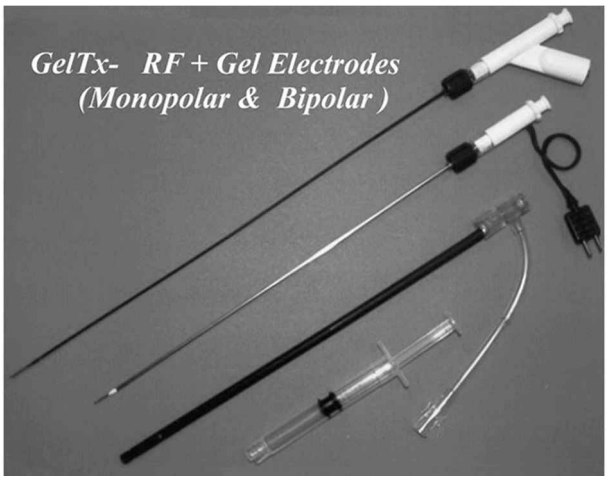

FIG. 3. Single RF needle electrode (**A**) monopolar and (**B**) bipolar.

Placement of needle electrodes and creation of lesion: For each treatment session, a single RF needle electrode was positioned at the center of the area to be ablated. The RF energy was delivered at 50 w at 500 kHz for 5 minutes. Generator output was slowly increased (over 2 minutes), so the tissue impedance increased very slowly. During RF, a hyperechoic area was observed around the electrode tip; after RF delivery stopped, the hyperechoic area slowly disappeared. A total of 12 monopolar and 6 bipolar lesions were created with the single needle electrode.

Chemoablative with and without monopolar and bipolar RF

Animals: Fifteen pigs were used.

Placement of needles and creation of lesion by hypertonic saline, ethanol, and acetic acid: A hollow insulated laparoscopic monopolar or bipolar RF needle electrode (18-gauge 2-cm exposed metal tip [GelTx™; Prosurge*Injectex*]) was placed in a predetermined area of the renal parenchyma under direct laparoscopic and ultrasound guidance for infusion of the specific gel. Hypertonic saline, ethanol, or acetic acid gel was infused through the needle electrode during ablation using the same RF settings (50 W at 500 kHz for 5 minutes) as were used for the aforedescribed plain RF trials. Generator output was slowly increased (over 2 minutes), so the tissue impedance increase slowly. Before activation of the electrode, 1 mL of hypertonic saline (23.4%), ethanol (95%), or acetic acid (50%) gel was injected; after activation of RF, continuous infusion of the selected chemoablative gel through the needle electrode into the renal parenchyma was continued at 2 mL/min (total 4 mL) into the area to be ablated. Ultrasonography (Tetrad system) was used to image the kidney before treatment, during injection, and after ablation, imaging being performed with a high-frequency 10-MHz transducer. During injection, a hyperechoic area was observed around the electrode tip; the patch progressively enlarged. After the treatment, the hyperechoic area slowly disappeared. Seven lesions were created with hypertonic saline gel (23.4%) and six each with ethanol gel (95%), acetic acid gel (50%), hypertonic saline gel with monopolar RF, hypertonic saline gel with bipolar RF, ethanol gel with monopolar RF, ethanol gel with bipolar RF, acetic acid gel with monopolar RF, and acetic acid gel with bipolar RF.

Heat-based radiofrequency energy

Animals: Three pigs were used.

Placement of probe and creation of lesion: The RF probe (StarBurst™ XL; RITA Medical Systems, Mountain View, CA) was designed to create a 3- or 5-cm lesion in the liver with 10 or 30 minutes of RF application, respectively (Fig. 4). For 3-cm lesions, the lateral tines are 2.5 apart, while for a 5-cm lesion, the lateral tines are 4.5 cm apart. The probe was placed under laparoscopic and ultrasound guidance; it was deployed under ultrasound guidance (Prosound™ 5000; Aloka Co., Wallingford, CT). Tissues were heated to $>100°C$ for 10 minutes using a Valleylab System 1500 with real-time temperature monitoring from five thermocouples within the array. The development of the lesion was monitored continuously with intracorporeal ultrasonography. To prevent bleeding, the needle track was closed using the track ablation mode of the system at the end of the procedure. Six lesions were created; one in each of the six kidneys. The tissues were harvested at 1 week and stained with H&E for histologic examination.

RESULTS

Cryotherapy

All animals completed the 1–week protocol. At sacrifice and harvest, various degrees of adhesions and inflammation were present on the kidney surface. Occasionally, some bowel adhesions were present at the site of the cryoablation, but no bowel damage was noted. There was no hemorrhage or urinoma.

Gross pathology: The capsule over the treatment site was thickened, occasionally wrinkled, and adherent to the underlying renal parenchyma. After removal of the renal capsule, the gross appearance of the lesion was regular. The treated parenchyma was grayish-white with a surrounding area of erythematous parenchyma for a few millimeters that merged into normal renal parenchyma. When the kidney was bivalved, it was noted that there was loss of the corticomedullary junction. The lesions were circular on the surface of the kidney and stopped at the renal pelvis. In a few animals, the renal pelvis was slightly thickened and pale but with no apparent erosion or perforation. The single-needle lesions averaged 33.0 (length) $\times$ 8.2 (breadth) $\times$ 8.2 mm (depth). The three-needle lesions averaged 23.5 $\times$ 20.3 $\times$ 13.9 mm (Table 1).

Histologic findings: Each lesion consisted of a wedge-shaped area of coagulative necrosis in the renal cortex and medulla extending to the renal pelvis (Fig. 5). The overlying renal capsule was thickened and fibrotic. There was a relatively abrupt transition (1–2 mm) at the border of the lesion from the necrotic to the viable tissue. The 1- to 2-mm intervening area revealed partial necrosis with hemorrhage, glomerular congestion and atrophy, segmental sclerosis, tubular necrosis, and capillary thrombosis. In the area of coagulative necrosis, there was a complete lack of cellular details for all kidney substructures extending from the renal capsule to the collecting ducts in the

FIG. 4. Heat-based RF system and StarBurst XL probe.

papilla. The urothelium of the renal pelvis revealed mucinous metaplasia in all animals. (Unlike the human, mucinous metaplasia of the urothelium is a common finding in the porcine model. In one animal, the urothelium was partially necrotic but still intact.) The margin of each of the lesions was infiltrated with polymorphonuclear leukocytes and some lymphocytes.

Microwave thermotherapy

All animals completed the 1-week protocol. At sacrifice and harvest, there were very few peritoneal adhesions. There were no adhesions between the bowel and the treated area.

Gross pathology: The lesion sites were smooth; the capsule was thickened and focally adherent to the underlying parenchyma. The lesion was grayish-white to yellow with a thin rim of surrounding pinkish renal parenchyma, which merged into normal parenchyma. There was evidence of some hemorrhage and a hole at the antennae site. The bivalved kidney revealed complete loss of the corticomedullary junction at the lesion site. The lesions were circular, extending equidistant from the antennae; the lesions extended to, but not through, the renal pelvis. The average lesion size was 22.0 × 17.3 × 11.0 mm (Table 1).

Histologic findings: There was coagulative necrosis in the renal cortex and medulla extending to the level of the renal pelvis (Fig. 6). The overlying renal capsule was slightly thickened by fibrosis. There was a very thin (≤1-mm) transition zone from the necrotic to the viable tissue. The urothelium of the renal pelvis was intact in all the animals. The necrotic zone at the margin of the lesion was infiltrated by polymorphonuclear leukocytes along with some lymphocytes.

Radiofrequency energy

All animals completed the 1–week protocol. Bubbles of gas and, occasionally, sparking from the electrosurgical probe were noted during activation of monopolar or bipolar RF; ultrasonography during RF revealed transient hyperechoic areas. At harvest, dense adhesions were consistently present on the renal surface. The peritoneum was also adherent at the site of the lesions. Occasionally, bowel was adherent at the renal treatment site. One pig had a urinoma.

Gross pathology: The site of the lesion was rough, thick, and adherent to the renal capsule. The lesions were pale yellow on the surface. There was some charring along the needle tract after both monopolar and bipolar RF. Within the lesion, there was loss of the corticomedullary junction. The lesion extended up to, but not into, the renal pelvis. With monopolar RF (N = 12), the lesions averaged 8.1 × 6.6 × 7.4 mm, while with

Table 1. Sizes of Ablative Lesions Created with Different Modalities

Technique	*No.*	*Length (mm ± SE)*	*Breadth (mm ± SE)*	*Depth (mm ± SE)*	*Complete necrosis (%)*
Microwaves (Urologix)	12	21.97 ± 2.12	17.25 ± 1.46	10.91 ± 0.35	12 (100)
Cryotherapy single microprobe (Galil)	10	8.33 ± 0.47	8.22 ± 0.52	8.22 ± 0.32	10 (100)
Cryotherapy three microprobes (Galil)	6	23.5 ± 1.73	20.25 ± 1.87	13.87 ± 0.72	6 (100)
RF (monopolar)	12	8.14 ± 1.33	6.57 ± 0.72	7.43 ± 0.92	11 (91.6)
RF (bipolar)	6	7.44 ± 1.02	6.44 ± 0.37	6.22 ± 0.57	5 (83.3)
Ethanol gel (95%)	6	4.8 ± 1.06	4 ± 0.31	4.6 ± 1.12	3 (50)
Ethanol gel + monopolar RF	6	12.2 ± 1.96	10 ± 0.31	8.0 ± 0.83	6 (100)
Ethanol gel + bipolar RF	6	10 ± 0.51	9.66 ± 0.33	7.66 ± 0.56	6 (100)
Hypertonic saline gel (23.4%)	7	2.33 ± 0.33	2 ± 0.0	1.66 ± 0.34	3 (50)
Hypertonic saline + monopolar RF	6	27 ± 4.37	22.2 ± 3.47	12.4 ± 1.69	6 (100)
Hypertonic saline + bipolar RF	6	21 ± 2	16.80 ± 1.82	12.2 ± 2.03	6 (100)
Acetic acid gel (50%)	6	14.4 ± 3.31	11.80 ± 2.53	7.4 ± 1.03	6 (100)
Acetic acid + monopolar RF	6	21.25 ± 2.05	17.25 ± 2.13	9.87 ± 0.95	6 (100)
Acetic acid + bipolar RF	6	20.33 ± 0.33	14 ± 3.05	9 ± 0.58	6 (100)
Heat-based RITA[a]	6	25.8 ± 0.20	23.1 ± 0.26	12.5 ± 0.11	6 (100)

[a]Measurements in cm.

bipolar RF (N = 6), the lesions averaged 7.4 × 6.4 × 6.2 mm (Table 1).

Histologic findings: Each lesion consisted of a wedge-shaped area of focal coagulative necrosis extending broadly from the renal cortex and the medulla to a narrower area at the level of the renal pelvis. In each case, the renal capsule overlying the lesion was firmly adherent and fibrotic. The lesions displayed a central zone of necrosis with a rim of inflammation (2–3 mm) and fibrosis at the border between the necrotic and viable tissue (Figs. 7 and 8). There was tubular hypereosinophilia and nuclear smudging with relative sparing of the glomeruli at the margin. One monopolar RF and one bipolar RF lesion contained skip areas of viable tissue.

Chemoablation with and without monopolar and bipolar RF

All animals completed the 1–week protocol after use of **hypertonic saline gel** with or without RF. At sacrifice and harvest, a few peritoneal adhesions were present on the kidney surface. There was no adherence between the bowel and the treated area. Occasionally, there was evidence of leakage of gel along

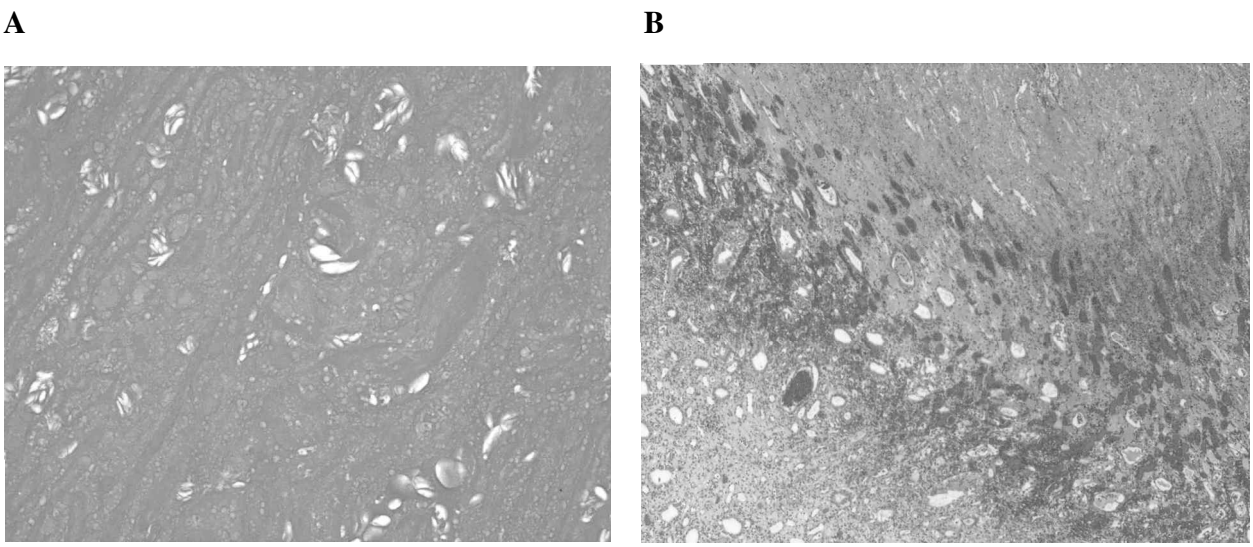

FIG. 5. Effects of cryoablation. (**A**) Lesion consists of coagulative necrosis of renal cortex and medulla. (**B**) Margin of cryolesion. There is relatively abrupt (1- to 2-mm) transition from necrotic to viable tissue. In this transition zone, there is partial necrosis with hemorrhage, glomerular congestion, and capillary thrombosis.

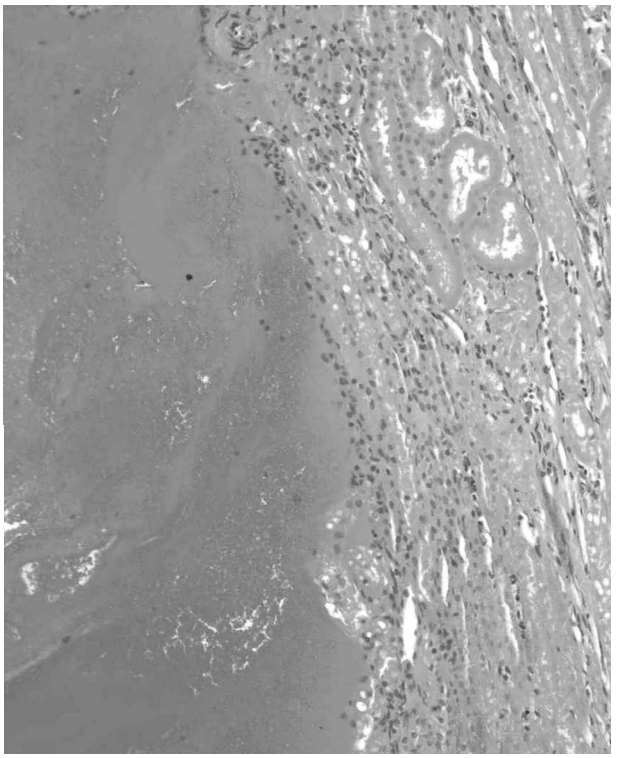

FIG. 6. Effects of microwave thermotherapy. Coagulative necrosis is seen in renal cortex and medulla with complete loss of details. Transition zone from necrotic to viable tissue is very thin (≤1mm).

the needle tract, especially when the needle was withdrawn quickly (the first two lesions created). To create the remaining lesions, we modified our surgical technique such that the needle was left in place for several minutes after gel injection and then slowly withdrawn; this maneuver seemed to limit or prevent back leakage of the gel. Leakage of hypertonic saline from the needle tract during RF activation caused superficial linear burn injuries to the renal surface.

Gross pathology: The lesions were cone shaped and irregular; in general, they were larger on the surface of the kidney and smaller toward the renal pelvis. The largest lesions were achieved using hypertonic saline gel with monopolar RF (27.0 × 22.2 × 12.4 mm) followed by hypertonic saline gel with bipolar RF (21.0 × 16.8 × 12.2 mm) (Table 1). The lesions created by hypertonic saline gel alone were small (2.33 ±.0.33 mm) and pale yellow.

Histologic findings: Each lesion consisted of a wedge-shaped area of focal coagulative necrosis extending broadly from the renal cortex and the medulla to a narrower area at the level of the renal pelvis (Fig. 9). The renal capsule overlying the lesion was normal after use of hypertonic saline alone, but after concomitant delivery of monopolar or bipolar RF energy, it was slightly thickened (Fig. 10). In three hypertonic saline lesions, there were skip areas of viable tissue; but there was complete necrosis with hypertonic saline injection plus monopolar or bipolar RF activation.

All animals treated with **ethanol gel** alone or with monopolar or bipolar RF completed the 1-week protocol. Occasionally, there had been leakage of ethanol gel along the needle tract. Serum ethanol concentrations at were 15.9 ± 1.80 mg/dL 1 hour and 11.8 ± 1.64 mg/dL at 3 hours. At harvest, marked peritoneal adhesions were present on the renal surface. In three animals, bowel was adherent to the treated area.

Gross pathology: Ethanol lesions were grossly wedge shaped, with irregular borders; the lesions were larger on the surface of the kidney and smaller toward the renal pelvis. Ethanol gel with monopolar RF produced lesions averaging 12.2 × 10 × 8.0 mm, while the lesions produced by ethanol gel with bipolar RF were slightly smaller: 10 × 9.7 × 7.7 mm. The lesions created by ethanol gel alone were only 4.8 × 4 × 4.6 mm (Table 1).

Histologic findings: Each lesion consisted of a wedge-shaped area of focal coagulative necrosis extending broadly from the renal cortex and the medulla to a narrower area at the level of the renal pelvis (Fig. 11). The renal capsule was slightly thickened in all cases, especially after treatment with monopolar or bipolar RF (Fig. 12). In three ethanol gel lesions, there were skip areas of viable tissue, but there was complete necrosis when monopolar or bipolar RF activation had also been used. Occasionally, when RF was used with ethanol, there were flames or smoke.

All animals treated with **acetic acid gel** with or without monopolar or bipolar RF completed the 1-week protocol. At sacrifice and harvest, marked peritoneal adhesions were present on the renal surface. In all animals, bowel was adherent to the treated renal surface. Occasionally, there was evidence of leakage of acetic acid gel along the needle tract. Arterial blood gas measurements were performed 1 and 3 hours after each procedure; the anion gap remained in the normal range, albeit in the upper region.

Gross pathology: Lesions created by acetic acid gel alone averaged 14.4 × 11.8 × 7.4 mm. Acetic acid gel with monopolar RF produced larger lesions: 21.3 × 17.3 × 17.3 mm, as did acetic acid gel combined with bipolar RF: 20.3 ×14 × 9 mm (Table 1).

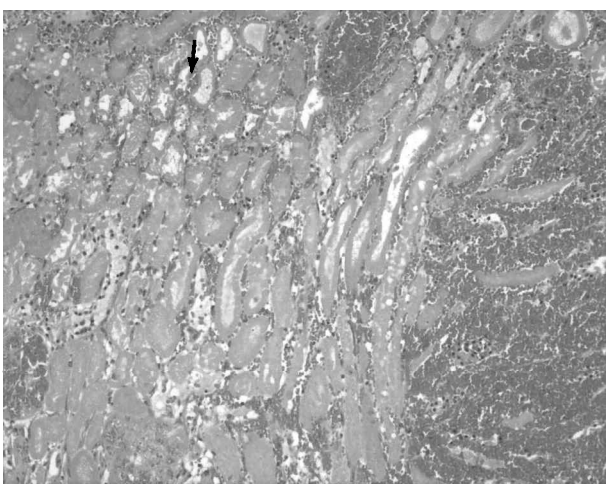

FIG. 7. Effects of monopolar RF energy. Lesions display central zone of necrosis with 2- to 3-mm rim of inflammation and fibrosis at the border between necrotic and viable tissue. Some viable cells are seen (arrow).

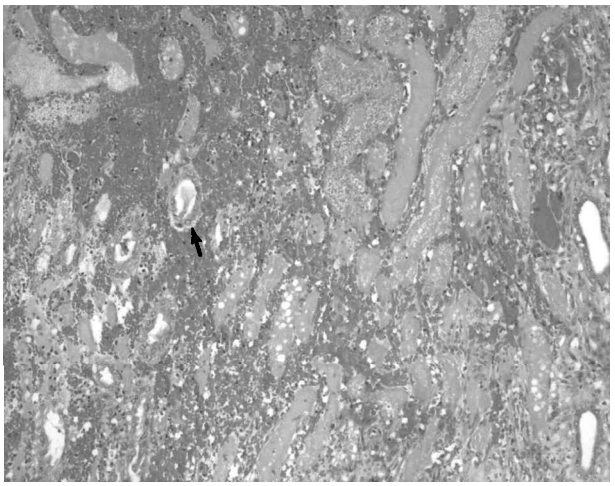

FIG. 8. Effects of bipolar RF energy. Lesions display central zone of necrosis with 1- to 3-mm rim of inflammation and fibrosis at border between necrotic and viable tissue. Some viable cells remain (arrow).

Histologic findings: The lesions produced were irregular in shape, larger on the surface of the kidney and smaller toward the renal pelvis. In all cases, with and without RF energy, the acetic acid gel was associated with complete necrosis without skip areas (Figs. 13 and 14). Acetic acid dissolved the renal capsule at the site of treatment and at any site of extravasation.

Heat-based RF treatment

All animals completed the 1-week protocol. At sacrifice and harvest, a few peritoneal adhesions were present on the kidney surface. In one animal, bowel was adherent to the treated area. The deployment of the needles was satisfactory in all six kidneys. On ultrasound imaging, the prongs were identified as hyperechoic dots; lesions were seen as hyperechoic areas emanating from the tips of the prongs.

Gross pathology The renal capsule overlying the lesion was firmly adherent and fibrotic. The lesions created averaged 2.6 × 2.3 × 1.3 cm (Table 1). The lesions were circular and pale yellow (Fig. 15). Within the lesion, there was loss of the corticomedullary junction. The lesion extended into the renal pelvis.

Histologic findings: There was complete necrosis with no skip areas, extending broadly from the renal cortex and the medulla (Fig. 16). The microscopic margin of the lesion was slightly dentate. There was a 2- to 3-mm rim of inflammation around the area of necrosis.

DISCUSSION

Cryotherapy

In urology, liquid nitrogen-based cryotherapy was first used in the 1960s for the treatment of prostate cancer[20]; however, it was abandoned because of the high complication rate secondary to failure to properly image probe placement prior to initiating the freezing process.[21] With the creation of argon-based cryosystems and the development of ultrasound imaging, cryotherapy has been reintroduced as a treatment for prostate cancer and small renal tumors. The new argon gas-based cryosurgical systems reach target temperatures quickly, and ultrasound monitoring allows real-time tracking of the freezing process. Although used in some centers, renal cryotherapy is still in its developmental phase. In this study, we used the smallest available cryoprobe (1.5 mm or 17 gauge) and applied it to the normal porcine kidney.

Mechanism of cryoinjury: Intense rapid freezing results in cellular death by several mechanisms.[22] Cell death during the **freezing cycle** has several causes: (1) a combination of intracellular and extracellular ice-crystal formation with subsequent rupture of plasma membranes, intracellular membranes, and organelles; (2) cellular dehydration; (3) protein denaturation; (4) hypoxia; (5) solute shifts; (6) uncoupling of oxidative phosphorylation; and (7) vascular thrombosis. In areas close to the cryoprobe, temperatures rapidly approach −165° to −190°C, depending on probe size. Farther away from the probe, temperatures drop less dramatically because of the vascular-based heat-sink effect; still, damage to tissue occurs because the cooling solutes are excluded from the forming ice, making the extracellular fluid hypertonic. As a result, nonfrozen tissue suffers damage secondary to the chemical gradient induced by dehydration. During the **thaw cycle**, additional tissue damage occurs as a result of acute vascular injury and the resulting hypoxia. Indeed, during the thaw cycle, smaller blood vessels rupture secondary to the chemical gradient that occurs within nonfrozen tissue. There is progressive damage to the microcirculation, resulting in hypoxia, endothelial cell damage, edema, and platelet aggregation with thrombosis and further vascular occlusion, all culminating in enhanced ischemic necrosis. In sum, whereas near the cryoprobe, extremely cold temperatures cause lethal intracellular ice crystal formation, at the periphery of the iceball, osmotic effects predominate.[23–25]

Intralesional temperature and tissue necrosis: It is generally accepted that the critical temperature to ensure cancer cell destruction is approximately −40°C.[26,27] It is postulated that a longer duration of freezing, repeated freeze-thaw cycles, and a longer thaw period may provide equal results at a slightly higher temperature.[22] Chosy and coworkers[28] used thermosensors to monitor the effects of cryotherapy on the kidney and

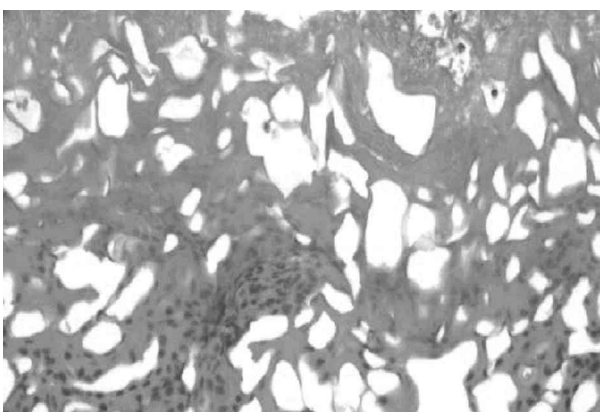

FIG. 9. Effects of hypertonic saline. Focal coagulative necrosis is apparent. There were skip areas of viable tissue in three of six lesions (50%).

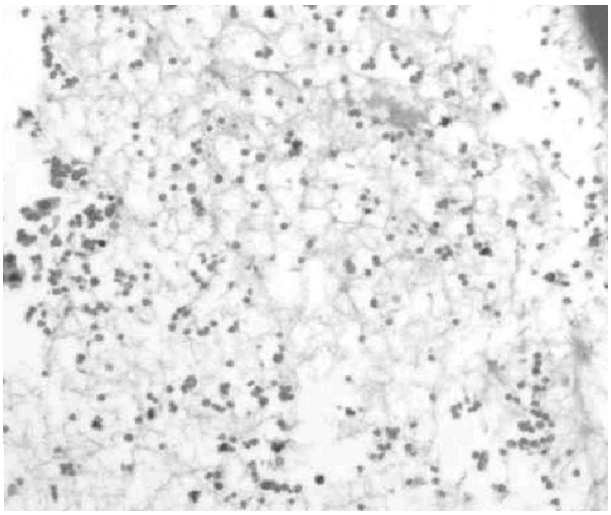

FIG. 10. Effects of hypertonic saline and monopolar RF energy. Each lesion consists of wedge-shaped area of focal coagulative necrosis extending broadly from renal cortex and medulla.

were able to corroborate the effectiveness of −20°C provided the freeze cycle lasted 15 minutes and a double-freeze technique was employed. Other factors that influence the size of the cryolesion include the area of contact between the cryoprobe and the targeted tissue and tissue vascularity. Increased blood flow creates a heat sink that may distort, while it slows, the symmetric growth of the iceball.[34] Of note, *ex vivo* ureteropyelograms and renal arteriograms in swine have demonstrated occlusive amputation of the collecting system and the vasculature of the ablated renal segment.[29]

During the first freeze, the rate and degree of blood flow are the most important determinants of the progress of the iceball. During subsequent freezes, changes in tissue-specific heat have a greater impact on the iceball size. While it may thus seem reasonable to clamp the renal artery during cryotherapy, occlusion of the renal blood flow does not in fact enhance the size of the cryolesion to a significant extent. Indeed, an intact circulation may protect the collecting system from injury.[30] Therefore, we did not occlude the blood supply of the kidney during our renal cryoablation trials.

Typically, the cryolesion develops very rapidly at first; indeed, most of the growth of the iceball occurs in the initial 5 minutes. Of note, while some studies have employed only a 5-minute freeze, other studies have shown that it takes approximately 20 minutes for the iceball to reach a steady state.[31]

Area of necrosis: It is important to determine the exact location within the iceball where reproducible and complete tissue necrosis occurs. During cryotherapy, incremental increases in temperature occur from the center toward the periphery of the lesion. As such, the advancing outer edge of the iceball is approximately 0°C, too high to cause cell death.[24] It is not until 4 to 6 mm inside the periphery of the iceball that the temperature is in the −20°C to −40°C range that is necessary for tissue necrosis.[32,33] Accordingly, it is important that the edge of the cryolesion, as seen laparoscopically and ultrasonography, extend approximately 1 cm beyond the visible margin of the targeted tumor.[34–36]

Fortunately, it appears that the renal pelvis is relatively resistant to cryotherapy. In our study, only one of seven animals had partial necrosis of the renal pelvis, and there was no defect or urinoma formation. These findings are similar to those of others,[37] who showed the effect of cryotherapy on the renal pelvis to be minimal. An acute lesion with sloughing of the urothelium and the lamina propria was noted; however, when animals were sacrificed at 1 month, there had been regrowth of the urothelium and lamina propria. This finding suggests that cryoablation could be used safely for hilar and centrally located renal tumors, but it remains unknown whether sufficient necrosis would occur because of the problem of the significant heat sink effect provided by the major renal vasculature in this area.

Because of the small size of the cryoprobes we used (i.e., 1.4 mm), we used both a single and multiple probes to see if the latter would allow the creation of larger lesions without skip areas. The three-probe deployment resulted in faster freezing with a reduction in the transition zone of ischemia and an almost threefold greater volume of treated area. However, even with triple-probe deployment, the lesion created was <8 cc, insufficient to fully treat a 2-cm lesion. We believe that if percutaneous therapy is to be effective, multiple-needle cryoprobes will be needed, perhaps as many as four to six on a template.

Histopathology findings: Sequential histologic changes after renal cryoablation are myriad. Within 1 hour, interstitial hemorrhage with vascular congestion is noted, accompanied by extravasation of red blood cells into the injured parenchyma and coagulative necrosis. At 1 week, four distinct zones are seen: central necrosis, inflammatory infiltrate, hemorrhage, and fibrosis.[38–40] Healing from cryoablation is gradual, occurring by secondary intention with steady fibrotic contracture of the involved area that produces a wedge-shaped chronic lesion.[28,38,41,42] At 1 week, we noted ischemic coagulative necrosis with a relatively abrupt (1- to 2-mm) transition from necrotic to viable tissue at the border of the lesion. There was hemorrhage in the transition zone. The urothelium of the renal pelvis was partially necrotic in one pig, but no urinoma formed. Urothelium in the renal pelvis showed evidence of mucinous

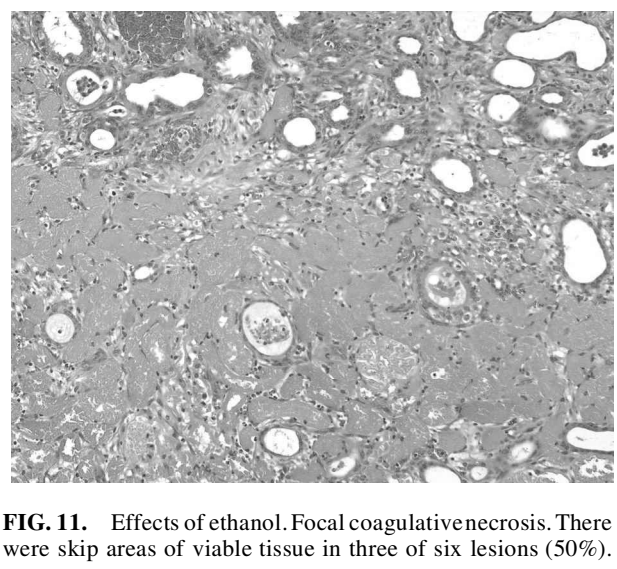

FIG. 11. Effects of ethanol. Focal coagulative necrosis. There were skip areas of viable tissue in three of six lesions (50%).

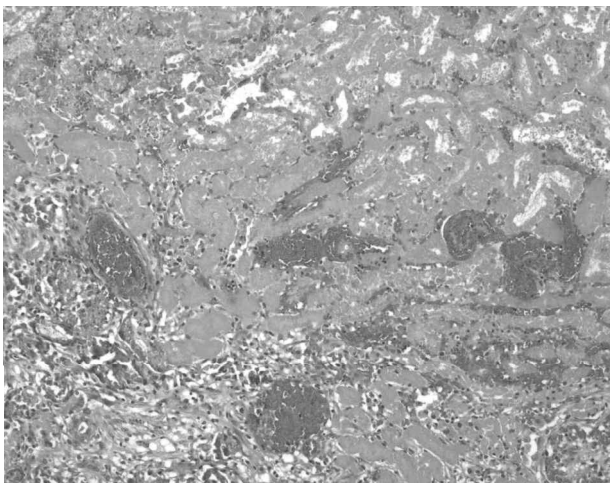

FIG. 12. Effects of ethanol with monopolar RF energy. Complete coagulative necrosis extends from renal cortex and medulla to renal pelvis.

metaplasia in all pigs, which is a common finding in this animal.[43]

Cryotherapy and bleeding: Cozzi and associates[41] reported 5 of 10 animals treated by cryoablation with 5-mm probes had subsequent hemorrhage following thaw. Tamponade of the tract was generally all that was necessary for hemostasis.[28,34,35,39,41,43,44] In contrast, perhaps because of the small size of the cryoprobes used in our study, we did not encounter any bleeding in any of our animals.

Cryotherapy and imaging: Renal ultrasonography effectively shows the formation of the anterior portion of the iceball, and because the cryolesion is spherical, its posterior extent can be inferred. Computed tomography has also been used to guide cryotherapy[45,46]; the iceball appears as a well-marginated low-attenuation area. Magnetic resonance imaging with an integrated guidance mechanism and MR-compatible cryoprobes can be used to show the iceball in its entirety[25,47–51] and can provide a three-dimensional image of the developing iceball. Also, the area of an iceball will no longer enhance with gadolinium.[47–53] On T_1-weighted images, all cryotherapy lesions are isointense with an occasional hyperintense rim; on T_2-weighted images, the lesions are hypointense. An MRI scan 1 month after surgery demonstrates an increase in signal intensity on both T_1- and T_2-weighted images but no enhancement. In follow-up after cryotherapy, sequential MRI scans are excellent for the detection of any changes in the treated lesion.[52]

Application of cryotherapy: Cryotherapy of the kidney may be delivered percutaneously or laparoscopically (Table 2). The former method, first described in 1995 by Uchida and colleagues,[54] was most recently updated and expanded by Shingleton and coworkers,[55] who imaged the lesion with an open MR scanner. Laparoscopic renal cryoablation has received a lot of attention lately from several centers. While far more invasive than a percutaneous approach, it has several potential benefits: ability to observe the margins of the iceball, ability to displace and protect adjacent structures, and potential control of hemorrhage. The clinical work of various investigators is summarized in Table 3. It has been proposed that a transperitoneal approach is better suited for anterior renal lesions; whereas a retroperitoneal approach affords better access to tumors on the posterior aspect of the kidney.[56] The entire laparoscopic procedure is monitored with an articulating laparoscopic transducer to ensure proper treatment of the tumor.[56–60] Injury to the bowel[29] and stricture of the ureteropelvic junction[30] have been reported after open cryoablation in a canine model; however, this has yet to occur clinically. Nonetheless, extreme care must be taken to monitor the iceball continuously under both laparoscopic vision and ultrasound imaging.

Microwave thermotherapy

Microwaves are the 300- to 3000-MHz range of the electromagnetic spectrum.[61] All waves in the microwave spectrum can interact with tissue and produce heat. For example, the Prostatron (EDAP-Technomed) uses a 1296-MHz frequency, while the T3 (Urologix) and Urowave (Dornier) use a 915-MHz frequency.[62] For surgical therapy, the microwaves are emitted from a flexible antenna. Microwave energy can be used for coagulation as well as ablation; it has been employed for hemostasis in open[63] and laparoscopic[64–67] partial nephrectomies. The flexibility of the microwave antenna and the coagulative nature of thermotherapy make the approach ideal for renal ablation. The depth of tissue penetration can be altered by changing the frequency of the energy source.

Mechanism of action: The microwaves emitted from the antenna (e.g., needle electrode) pass through the tissue and create a rapidly alternating electromagnetic field that leads to oscillation of free charges (electrons and ions). As the water molecules follow the changing polarity of the field, the increased kinetic energy is transformed into heat, resulting in coagulation necrosis.[61] The tissue temperatures in a microwave field depend, not only on the energy imparted to the tissue, but also on the thermal conduction and convection, which are related to tissue perfusion and tissue heterogeneity.[68] The depth of penetration is inversely related to the frequency and the water content of the targeted tissue.[69] At any time, tissue penetration also varies directly with temperature. Thus, accurate tis-

FIG. 13. Effects of acetic acid. There was complete coagulative necrosis with 100% cell kill in all lesions. Lesions display central zone of necrosis and hemorrhage.

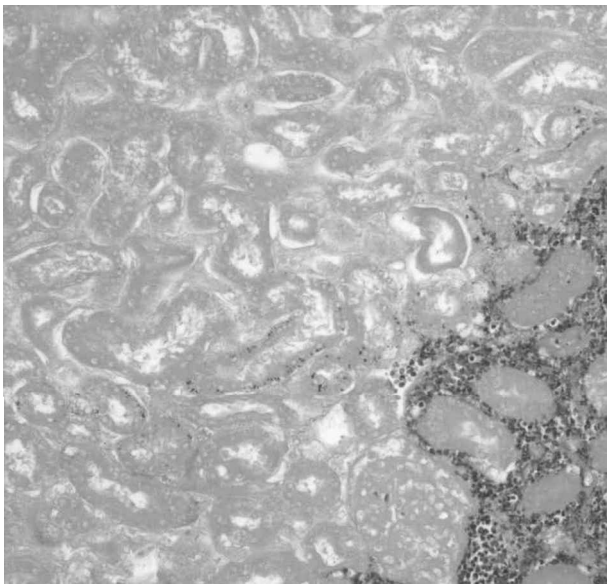

FIG. 14. Effects of acetic acid and monopolar RF energy. Lesions were irregular, larger on surface of kidney and smaller toward renal pelvis. There was complete necrosis without skip areas.

sue temperature monitoring is paramount to successful and safe MT. Maintaining intralesional temperatures at >45°C while simultaneously keeping the surrounding temperatures <45°C will cause coagulation necrosis in the targeted lesion while preserving the surrounding normal tissue.[70–73]

Temperature correlation: At 40°C, cellular homeostasis is maintained; however, at 42° to 45°C (hyperthermia), cells become susceptible to damage.[74,75] However, even prolonged heating at these temperatures will not result in complete cell death in a given volume of tissue. When temperatures are increased further, to ≥46°C (i.e., thermotherapy) for 60 minutes, irreversible cellular damage will occur.[76] Increasing the temperature only a few degrees further, to 50° to 52°C, markedly shortens the required treatment time (4–6 minutes).[77] Between 60° and 100°C, nearly instantaneous coagulation of cytosolic and mitochondrial enzymes and nucleic acid–histone complexes occurs.[78] After thermal damage, cells undergo coagulative necrosis over the course of several days. Temperatures >105°C result in tissue boiling, vaporization, and carbonization. This process actually retards the spread of necrosis because of a decrease in energy transmission.[77] Thus, for ablative thermotherapy, the goal is to achieve and maintain a 50° to 100°C range within the entire target volume without causing carbonization. In addition, tissue with increased blood flow may be less susceptible to heat injury because of the heat-sink effect.[79–82]

Creation of bigger lesions: During microwave treatment, tissue temperature is measured via fiberoptic thermosensors located different distances from the microwave antenna. Thermotherapy with a quick rise in temperature (i.e., "heat shock") is more effective than slow heating, as the rapid rise in temperature (in 4 to 6 minutes) causes early vascular thrombosis and subsequent coagulation necrosis.[83] Also, the rapid rise in temperature precludes the inhibition of thermotherapy by vasodilatation and concomitant augmentation of the heat-sink effect.[76] Lastly, the treatment times are reduced using the heat-shock approach.[84]

Effect of different antennae: In addition to the microwave generator's power and the heat-shock strategy, the configuration of the interstitial antenna is of significant importance for achieving adequate intralesional tissue temperatures.[85] To achieve high temperatures, the antenna must have minimal back heating and reflected power.[72,85,86] Monopole antennas (Prostatron) reflect 15% of their energy back to the antenna, so the energy absorbed by tissue is less; in contrast, a dipole antenna reflects only 1% of the energy.[86] In the present study, we used a dipole antenna. Also, proper function of the microwave antenna is dependent on proper impedance matching, which in turn is dependent on the dielectric properties of the tissue surrounding the antenna. Highly perfused tissues, such as the kidney, have a high water content; water has a high dielectric constant. If water is driven out of the tissue by excessive heating, the dielectric constant will change dramatically, causing the resonance of the antenna to move upward beyond the capability of the antenna to achieve efficient transfer of energy.

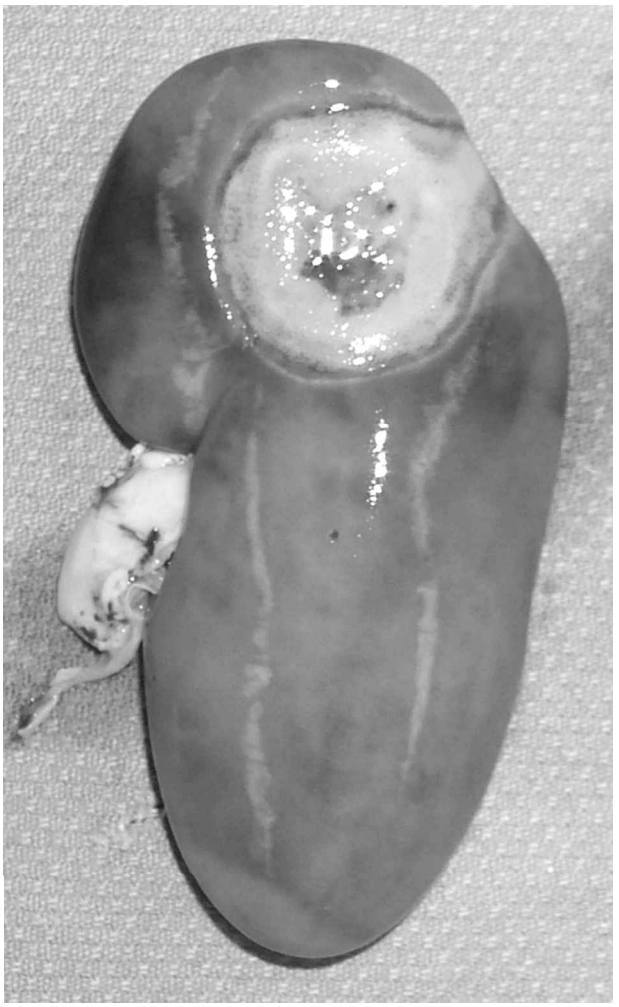

FIG. 15. Gross appearance of heat-based RF (RITA)-induced lesion. Lesions are circular and pale yellow. Within lesion, there is loss of corticomedullary junction.

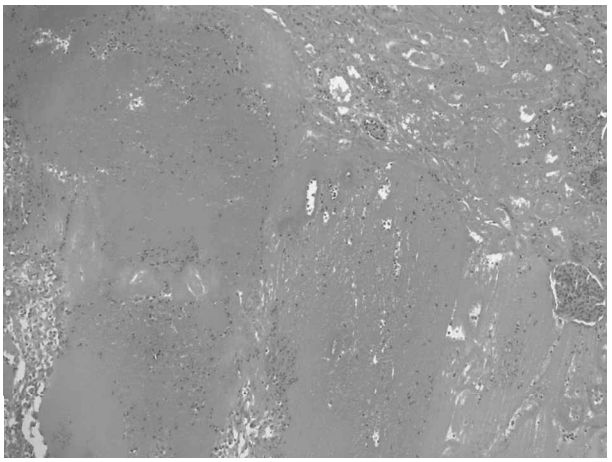

FIG. 16. Histologic effects of heat-based RF (RITA)-induced lesion. Complete necrosis with no skip areas is seen to extend broadly from renal cortex and medulla. Microscopic margin of lesion is slightly dentate. There is 2- to 3-mm rim of inflammation around area of necrosis.

Literature review: microwave renal ablation: The first experimental studies on renal ablative MT were performed in rabbit kidneys. Kigure and associates reported on the laparoscopic application of MT in an *in vivo* VX-2 tumor model implanted in rabbit kidneys (Table 4).[67] Their report showed no difference in survival between rabbits treated with laparoscopic MT and those undergoing open nephrectomy. The initial studies demonstrated the ability of MT to cause coagulative necrosis 5 mm from the electrode; temperatures >60°C were routinely recorded.[63] Furthermore, there was no significant elevation of temperature 2 cm from the electrode. Later studies of percutaneous ultrasound-guided treatment of implanted VX-2 carcinoma with MT confirmed the effectiveness of this modality.[67]

Radiofrequency energy (monopolar and bipolar)

Clark in 1911 first published on the use of RF energy (high-frequency alternating current) to cut and coagulate living tissue, including bladder tumors.[87] Radiofrequency energy became popular in surgery after the pioneering work of Harvey Cushing, a neurosurgeon, and W. T. Bovie, a physicist.[88] Advances have been made in the methodology of modulating the RF waveform, controlling the power output, and monitoring the electrode tip temperature. These changes have enabled wider application of RF current in all surgical specialties.

The equipment required for RF ablation is a generator, a probe, and a grounding pad; in addition, for ablation therapy, it is recommend to have available a data recorder (computer with software to record thermocouple temperatures, impedance, and the amount of power and energy delivered). The RF generators are similar in appearance to those in common use for electrosurgical cutting and coagulation in today's operating room. Most RF generators deliver a 300-kHz to 500-MHz continuous unmodulated sinusoidal waveform and are designed to reduce interference from other electronic equipment.

Soft-tissue ablation using RF energy has been widely practiced during open and endoscopic procedures. The objective is to create the largest lesion using the smallest possible electrode size and minimum RF power. This can be achieved by minimizing the power density around the electrode, which can be accomplished by increasing the conductivity of the tissue (i.e., reducing the tissue impedance) surrounding the electrode. The goal of RF tumor ablation is to treat for 5 mm beyond the targeted lesion in order to achieve satisfactory margins.

Mechanism of action: The RF energy travels from the active (positive) electrode to return to either the patient's grounding plate (negative) electrode (monopolar) or a negative electrode built into the delivery needle (bipolar).[89–92] The RF current flows from the needle electrode into the surrounding tissue on its way to the grounding pad; this causes agitation of water molecules, which creates molecular friction at the cellular level, thereby producing heat.[93] The cellular fluid in the tissue (0.9% saline) readily conducts the RF current; however, over time, the tissue impedance increases. Eventually, the cellular and extracellular fluid reach the boiling point, the end result of which is tissue necrosis secondary to protein denaturation, desiccation, and coagulation. This form of RF application differs from direct heating of tissue by a "hot" probe, as would occur with electrocautery; instead, the tissue surrounding the electrode, rather than the electrode itself, is the primary source of heat production.[93,94] Animal studies have shown that RF energy can be delivered with an adequate density per unit volume of neoplastic tissue.[89]

As the target tissue temperature increases to approximately 50°C, cellular proteins become denatured, and the cellular lipid component begins to melt, leading to disintegration of cell membranes and irreversible tissue destruction (normal tissue). It is generally thought that temperatures >70° to 80°C need to be reached for tumor ablation. Both a rapid fall-off of energy from the probe and poor heat conduction adversely affect the lesion size. The heat energy that can be deposited in the tissues is limited by tissue boiling and vaporization at higher temperatures (>105°C). When tissue vaporizes, gas is formed, which both increases tissue impedance, thereby reducing the extent of heat spread in the tissue, and serves as an insulator, thereby decreasing heat and current spread.

With monopolar RF energy, a large portion of the patient becomes part of the circuit as electrons flow from the point at which they are delivered by the needle electrode to the ground or return plate. The risk of accidental burns is higher because electrons seek the path of least resistance, and if the return pad is faulty, the current may exit other areas of the body. In contrast, bipolar RF is essentially a miniaturized isolated circuit, in which the active electrode (source of the current) and receiving electrode are located on the same needle. The current therefore does not travel through the body to a return plate but only through the tissue between the electrodes. The patient does not become a part of the circuit: only the tissue between the electrodes does. Bipolar systems have greatly reduced the hazards secondary to stray current.

Variables: There have been a number of approaches to creating larger RF lesions: increasing the effective size of the electrode,[90,91,95,96] cooling the electrode tip with a circulating fluid, using multiple probes or multiple-prong electrodes, and lowering the impedance of the tissue surrounding the electrode by infusing the periprobe area with a conducting solution.[90,97]

Table 2. Animal Studies of Cryotherapy of Kidney

Series (year)	*Subjects*	*Approach*	*Technique*	*Pertinent aspects*
Bush et al[142] (1964)	Rat	Open	Direct submersion in liquid nitrogen	Renal function recovery after rapid cooling with liquid nitrogen
Breining et al[143] (1974)	Rats	Open	Direct contact	Histologic, histochemical, and autoradiographic analysis
Helpap et al[144] (1979)	Rats	Open	Direct contact (6.5 mm^2)	Immunologic response
Sindelar et al[42] (1981)	Rat	Open	Puncture	Ultrastructural changes during renal cryoablation and monitoring of iceball
Barone and Rodgers[145] (1988)	Rabbits	Open	Puncture	Functional and morphologic effects
Onik et al[146] (1993)	Dog	Open	Puncture	Ultrasound characteristics
Stephenson et al[40] (1996)	Dogs	Open, laparoscopic	Contact	Laparoscopic cryoablation (single freeze cycle)
Cozzi et al[41] (1996)	Sheep	Open	Puncture	Open cryoablation (single freeze cycle)
Gill et al[29] (1996)	Pigs	Laparoscopic	Puncture	Laparoscopic/percutaneous cryoablation
Chosy et al[28] (1996)	Pigs	Open	Puncture	Thermosensor-monitored cryotherapy
Nakada et al[39] (1997)	Pigs	Laparoscopic	Puncture	Puncture *v* contact
Campbell et al[30] (1998)	Dogs	Open	Puncture	Impact of renal artery clamping
Sung et al[147] (1999)	Pigs	Open	Puncture	Impact of cryoablation on collecting system
Chen et al[148] (1999)	Pigs	Open	Puncture	Doppler flow and power Doppler studies after cryoablation
Nakada et al[149] (1999)	Rabbit	Open	Puncture	Therapeutic efficacy in implanted VX2 tumor model *v* nephrectomy
Present study (2001)	Porcine	Laparoscopic	Puncture	Feasibility of using ultrasmall (1.4-mm) cryoprobes to reduced hemorrhage and enhance percutaneous therapy

Also, the time of application directly impacts the extent of the lesion created (Table 5).

Increasing RF energy deposition: probe number: The use of multiple probes or of a single probe with multiple tines greatly increases the extent of ablated tissue. In an *in vivo* study on calf livers, Goldberg and colleagues[98] produced uniform spherical necrosis using three or four probes placed in close proximity; lesions measured 3.0 ± 0.2 cm and 3.2 ± 0.1 cm, respectively. Probes produced overlapping lesions if they were within 1.5 cm of each other.[98]

Improving RF energy delivery to the tissue: Wet RF: By infusing a small quantity of isotonic saline into the targeted tissue via the needle electrode, the conductivity of the tissue can be improved, allowing RF energy to be conducted for a longer time and hence to cause a larger zone of necrosis.[89,99] The infusion of saline blunts the rise in tissue impedance by increasing the conductivity of the extracellular fluid.[99–102]

In a study comparing conventional RF (without saline perfusion) and RF with saline perfusion (14.6% sodium chloride) in the dog prostate, Hoey and colleagues[103] demonstrated that RF with saline pretreatment created bigger lesions (mean 8.5 cm) than conventional RF (mean 0.34 cm).[89,91] Usually, a hypertonic saline infusion of only 1 mL/min (wet RF) is infused during the RF activation.[89,103–106] By increasing the duration of RF energy (with power and electrolyte concentration held constant), the size of the lesion can be extended to several centimeters.[105]

Tissue conductivity can be further increased by infusing hypertonic saline (23.6%). The advantage of using hypertonic saline is that smaller amounts of fluid can be infused (e.g., 4 mL). This prevents the creation of too large a lesion.

One drawback of using saline is that it has the tendency to leak around the RF needle as it is infused. In order to limit this problem, we created a hypertonic saline conducting gel. With the gel, the lesion is more localized and flow back along the needle also appears to be decreased.

Table 3. Clinical Studies of Cryotherapy of Kidney

Series (year)	*Subjects (no.)*	*Approach*	*Technique*	*Pertinent aspects*
Uchida et al[54] (1995)	Dogs, human (2)	Percutaneous	Puncture	Percutaneous renal cryoablation; embolized kidney to prevent rewarming from circulating blood showing increased efficacy of tumor kill
Delworth et al[150] (1996)	Human (2)	Open	Puncture	Open renal cryoablation of a central RCC, with success at 1-month follow-up.
Gill et al[56] (1998)	Human (10)	Laparoscopic	Puncture	Laparoscopic renal cryoablation
McGinnis et al[151] (1998)	Pigs Human (3)	Laparoscopic	Puncture	Laparoscopic cryoablation (retroperitoneal) is feasible
Bishoff et al[38] (1999)	Pigs Human (8)	Laparoscopic	Puncture	Pig laparoscopic cryoablation ($N = 12$); human laparoscopic cryoablation ($N = 8$)
Orihuela et al[152] (1999)	Human (15)	Open (just before nephrectomy)	Puncture	Prenephrectomy cryoablation with artery clamping has no effect
Gill et al[153] (2000)	Human (32)	Laparoscopic	Puncture	Retroperitoneal and transperitoneal cryotherapy. Postcryotherapy biopsies used for follow-up at 3 and 6 months
Shingleton et al[55] (2001)	Human (20)	Percutaneous	Puncture	MRI-guided percutaneous cryotherapy ($N = 22$)
Steinberg et al (Gill)[154] (2002)	Human (36) 22 (61%) positive biopsy	Laparoscopic	Puncture	Retroperitoneal and transperitoneal cryotherapy. Postcryotherapy biopsies used for follow-up at 3 and 6 months; 24 patients >4-year follow-up. Biopsy at 6 months negative; 1 (2%) had enhancing mass at 18 months and biopsy-confirmed recurrent RCC
Shingleton et al[155] (2003)	Human ($N = 70$) with 70 lesions	Percutaneous (open MRI)	Puncture	Renal tumor ≤5 cm Triple freeze and thaw cycle, with 5-mm margin, 2–4 probes used Follow-up 2 years (1–3.5 years) Retreatment 13%

In our study, the conductive gel provided efficient RF energy transfer while simultaneously cooling the electrode tip. The resultant effect was much larger lesions without increasing the size of the electrode. The largest lesions were achieved using hypertonic saline gel with monopolar RF (27 ± 4.3 mm) followed by hypertonic saline gel with bipolar RF (21 ± 2 mm). There were no skip areas in these lesions.

Imaging: Using ultrasound, RF was seen as a hyperechoic area, which slowly disappeared over 30 minutes following RF treatment.[107] A good correlation has been shown between hyperechoic areas and subsequent necrosis; however, the edge of the echogenic region remained irregular and ill defined.[107] On contrast-enhanced CT or MRI, the chronic changes of RF (i.e., coagulation necrosis) appear as a new area of nonenhancement; there is often a 2- to 3-mm peripheral enhancing rim seen both on gadolinium-enhanced MRI and, albeit more rarely, contrast-enhanced CT. This area has been shown by pathologic evaluation to correlate with a rim of granulation tissue. Indeed, absence of a well-defined rim may be indicative of residual tumor and necessitates biopsy.

Literature review: RF for renal ablation: Zlotta and colleagues first described use of RF for renal tumors (Tables 6 and 7). Initially, they used RF on nephrectomy specimens immediately *ex vivo* and then did *in vivo* RF for <3-cm lesions just prior to nephrectomy.[108,109] The RF lesions were $2.2 \times 3 \times 2.5$ cm. Histologic examination revealed intense stromal and ep-

Table 4. Literature Review of Microwave Thermotherapy of Kidney

Series (year)	*Subjects*	*Tissue (No.)*	*Approach*	*Size of lesion*	*Pertinent aspects*
Kigure et al[63,156] (1994, 1995)	Rabbit	VX 2 rabbit renal tumor (18)	Percutaneous (ultrasound guided)	5-mm area of coagulation necrosis (1 week and 8 weeks)	2450 MHz at 100 W for 30 s; histologic examination revealed complete coagulation necrosis
Kigure et al[67] (1996)	Rabbit	VX 2 rabbit renal tumor (10)	Laparoscopic	5–6-mm coagulative necrosis around probe, which was further surrounded by 5-mm area of scattered hemorrhage (2 weeks)	2450-MHz microwaves at 100 W for 30 s
Present study (2001)	Pig	Normal kidney (12)	Laparoscopic	22-mm area of coagulative necrosis (1 week)	915 MHz at 20 W for 15 min; histologic examination revealed complete coagulation necrosis.

Clinically, microwave thermotherapy has been used to control hemostasis during partial nephrectomy,[157,158] but complete ablation of the lesion has not been performed. Urologix has introduced new antennae, and a different setting creates much larger lesion (Eric Rudie, personal communication).

ithelial edema, as well as marked pyknosis and peripheral hemorrhage in all lesions. Pathologic review showed extensive coagulative necrosis of the lesion with no residual tumor cells. No damage was noted beyond the targeted area. Normal renal cells were affected in much the same way as tumor cells. Subsequently, McGovern and associates[110] treated renal tumors percutaneously with standard RF with the patients under intravenous sedation and saw no evidence of lesion enhancement at 3-month follow-up by CT scans. Sullman and colleagues[111] treated two patients with renal masses using MRI-guided RF ablation percutaneously. Pavlovich and Walther and their coworkers reported percutaneous treatment of two patients with Von Hippel-Lindau disease using RF ablation under CT and ultrasound guidance.[112,113] Lesions as large as 2.9 cm were ablated. Follow-up CT scans showed no lesion enhancement. However, more recently, there have been three clinical studies[114–117] showing persistence of some viable cells within the tumor after RF. Our findings are compatible with these more ominous observations of viable skip areas or peripheral viable tumor. The dry RF techniques tested in our study produced cellular necrosis on normal porcine renal parenchyma but left skip areas in some of the lesions; however, the addition of hypertonic saline conduction gel with both monopolar and bipolar RF (i.e., wet RF) created larger lesions with complete necrosis. This has been observed clinically as well when tumor was ablated with wet RF before partial nephrectomy (Dr. J. Libertino, personal communication).

Lastly, there is evidence that "cooled-tip" electrodes (continuous flow of ice-cold fluid in needle electrode) coupled with a high-energy-output generator (220 W) preclude a sudden rise in impedance and thus may be more effective.[118,119] At the National Cancer Institute, Walther and colleagues have used a cooled-tip 200-W RFA generator (Radionics, Burlington, MA) for renal radiofrequency ablation since 2001 (Marston Linehan, personal communication). A total of 8 and 12 hereditary-type renal tumors have been ablated percutaneously and laparoscopically. At a median follow-up of 384 days, none of the ablated tumors demonstrated contrast enhancement on CT imaging, so the patients are considered recurrence free by CT criteria.

Table 5. RF Parameters Affecting Size of Lesion

Parameters for lesion formation	Power (W), electrode size (area), treatment time, tissue impedance (Ω), power density (power area), energy density (power density × treatment time)
Power density (PD) (power/area)	Higher PD creates rapid, albeit smaller, lesions, while lower PD creates larger lesions over time.
Tissue impedance	Higher impedance (less conduction) creates smaller lesions; lower impedance allows bigger lesions to be created.
Electrode size	Smaller electrodes create smaller lesions; bigger electrodes create larger lesions.
Treatment time	Shorter treatment time creates a smaller lesion, while a longer treatment time creates a larger lesion.

Table 6. Review of RF Renal Ablation (Animal Studies)

Series (year)	Subjects (No.)	Tissue	Approach	Lesion size	Pertinent aspects
Polascik et al[159] (1999)	Rabbit (9)	VX-2 tumor	Open under US guidance	1.4 × 1 cm (30 sec) 1.8 × 1.5 cm (45 sec)	Interstitial single-augmented RF of nonmalignant (control) and malignant (the VX2 tumor) tissues under US guidance in renal tissue in a rabbit model 50 W at 500 KHz for 30 to 45 sec
Merkle et al[160] (1999)	Pig (3)	Normal tissue	Percutaneous (MR guidance)	7–14 mm	120 W at 500 KHz for 10 min
Patel et al[106] (2000)	Rabbit (48)	Normal tissue	Laparoscopic; needle placed percutaneously	7 cm (1 min) 10 cm (2 min)	Interstitial saline-augmented RF 50 W at 475 KHz for 1 or 2 min
Nakada et al[161] (2000)	Rabbit (30)	VX 2 tumor implanted in kidney	Open	N/A	Therapeutic efficacy in implanted VX2 tumor model with multitine 12-gauge RF probe; 90°C for 8 min (RITA Medical) compared with nephrectomy for treatment; therapies found to be equally efficacious.
Gill et al[162,163] (2000)	Pig: acute (6) and chronic (5)	Normal tissue	Laparoscopic (acute) Percutaneous (chronic)	3 × 1.5 (day 7) Lesion reabsorbed and replaced by scar at 1 month	55 W for 5 min then increased incrementally by 10 W every minute until impedance of 100 Ω was reached. Multitine probe. Complete necrosis.
Present study (2001)	Pig (20)	Parenchyma	Laparoscopic	Monopolar 8.14 × 6.57 × 7.43 mm Bipolar 7.44 × 6.44 × 6.22 mm	Both dry and wet (i.e., infusion of 23.4% saline gel) via single probe

Hypertonic saline gel

In the early 1990s, hypertonic saline infusion was used to treat benign liver cysts. Hypertonic saline has recently been used to treat hepatocellular carcinoma (HCC),[120] liver cysts,[121] and benign prostatic tissue. Likewise, it has been used to sclerose telangiectasias.[122–126] The most recent interest in the use of hypertonic saline injection has been as an adjunct to RF energy; the injected hypertonic saline allows greater spread of the energy. In this regard, much work has been done by Hoey, Leveillee, and colleagues in the prostate.

Mechanism of action: Normal and hypertonic (14.6%) saline have been used.[122,105] Hypertonic saline is helpful as it has a direct cytotoxic effect by virtue of its osmotic action, which causes cellular dehydration. We have used 23.4% saline in our studies, as the higher concentration minimizes the volume needed (e.g., 4 mL instead of 15–20 mL).

Renal ablation: The present study is the first to use hypertonic saline as a stand-alone therapeutic agent for renal ablation. We first characterized and compared the volume, regularity, and histologic manifestations of renal lesions produced by the injection of 23.4% saline immediately postoperatively and at 48 hours. In this group of animals, a small quantity of indigo carmine was added to each injected volume to delineate the extent of the agent's diffusion. There was uncontrolled leakage from the needle tract; accordingly, we designed a hypertonic saline gel to limit the leakage. However, the lesions created with hypertonic saline gel alone remained small (2.33 ± 0.33 mm) and were characterized by the presence of skip areas of viable tissue.

Ethanol gel with or without single monopolar and bipolar RF

Ethanol has been employed in transarterial embolization in patients with renal-cell carcinoma since the early 1980s[127–129] or just prior to planned radical nephrectomy to reduce collateral flow through tumor vessels.[127–129] Iaccarino used percutaneous ethanol injection into the renal vasculature (transarterial) for renal hypertension in patients unsuitable for angioplasty or surgery. Similarly, ethanol injection has been used for many years for renal cyst sclerotherapy.

Ethanol was first used for ablation of a parenchymal hepatic tumor in 1983 in Japan; it was administered under real-time ultrasound guidance.[130] Absolute ethanol injection resulted in extensive tumor destruction and marked reduction in tumor vascularity.[131] Since then, the use of hepatic tumor ethanol injection has become more widespread; however, to date, there

TABLE 7. REVIEW OF RF RENAL TUMOR ABLATION (HUMAN STUDIES)

Series (year)	*No.*	*Approach*	*Lesion size (cm)*	*Pertinent aspects*
Hall et al[164] (2000)	1	Percutaneous (CT guided)		Combined embolization (interlobar artery) and RF. Three RF activations were given: 60 W/4 min, 60 W/3 min, 50 W/5 min.
Sullmann et al[111] (2000)	2	Percutaneous (MR guided)	2–3.5	1.5 amp for 30 min
Pavlovich et al[112] (2000)	2 (VHL or HPRC)[a]	Percutaneous (combined ultrasound and CT guided)	2.4–2.9	26 w, 480 KHz for 5 minutes (temperature (95 to 105°C)
Geravis et al[165] (2000)	9 (7 biopsy proven; 2 enhancing lesions; mean 3.3 cm (1.2–5 cm)	Percutaneous	<3 (1RF cycle)	Free of enhancement
			>3 (>1 RF cycle)	4/6 free of enhancement Follow-up 10.3 months Cool-tip electrode 1500–1800 milliamp for 1 min Pulsing to prevent sudden rise impedance
Pavlovich et al[166] (2002)	21	Percutaneous	2 RF cycles 19/24 temp >70°C 5/24 temp <70°C (2-month CT data presented)	19/24 tumors ceased to enhance
Walther et al[113] (2000)	Phase II study in 4 pts with 11 tumors	Open	Tumor <5 cm treated	10/11 lesions completely treated (26 W, 480 KHz for 5 min; temp 95° to 105°C)
Zlotta et al[108,109] (1996, 1997)	*Ex vivo* (4); *in vivo* (2)	*Ex vivo* (after kidney removed) and *in vivo* (just before open nephrectomy)	2.2 × 3 × 2.5	*Ex vivo*, maximum temperature at needle tip ranged from 84° to 130°C with 10 to 14 W applied over 10 to 14 min
McGovern et al[110] (1999)	1	Percutaneous	Case report	Tumor heated to 90°C for 1 min at 500 KHz followed by 1200 milliamp for 12 min
Matlaga et al[167] (2002)	10 (tumor excised after ablation)	Open surgery, ultrasound guided	3.2 (1.4–8)	8 completely ablated with 200 W for 12 min Pulsing to prevent sudden rise in impedance 18-gauge probe (one probe for tumor <2 cm and three probes for tumor >2 cm Cool-tip electrode
Rendon et al[117] (2002)	10 (9 biopsy proven; 1 angiomyo[a]) Acue ($N = 4$) nephrectomy after treatment; chronic ($N = 6$) nephrectomy at 1 week	Open surgery, CT or US guided	2.4	1/5 acute group totally ablated 3/6 delayed group totally ablated 2 cycles applied LeVeen electrode (Radiotherapeutics)
Michaels et al[168] (2002)	15 pts with 20 tumors	Open (ablation before partial nephrectomy; US monitoring	2.4 (1.5–3.5)	110 watts at 460 KHz for 6–16 minutes (heated to 90–110°C) (RITA StarBurst XL probe, RITA Medical, California)
De Baere et al[119] (2002)	5	Percutaneous CT or US	3.3 (3.0–4.0)	480 KHz generator at 200 W; 15-min treatment cycle; one or two treatment cycles Cool-tip electrode
Gervais et al[118] (2003)	34 pts with 42 tumors	Percutaneous	3.2 (1.1–5)	200 W generator; 12-min treatment cycle Cool-tip electrode Mean follow-up 13.2 mos

[a]VHL = Von Hippel-Lindau disease; HPRC = hereditary papillary renal-cell carcinoma; angiomyo = angiomyolipoma.

are no data on using this modality for the treatment of small solid renal tumors.

Mechanism of action: Animal studies have shown the toxic effects of alcohol at the cellular level.[132–137] Specifically, alcohol diffuses into cells and produces an immediate coagulation necrosis secondary to dehydration, membrane lysis, and protein denaturation. The chronic effects of this exposure are fibrosis and small-vessel occlusion/thrombosis. The end result is marked cell necrosis.

Renal ablation: To the best of our knowledge, ours is the first report of the use of direct ethanol injection to ablate renal parenchyma. We characterized and compared the volume, regularity, and histologic appearance of renal lesions produced by injection of 95% ethanol immediately postoperatively and at 48 hours. In this group of animals, a small quantity of indigo carmine was added to each injected volume to delineate the extent of the agent's diffusion. Our initial results showed that ethanol diffused into the tissues in an uncontrolled manner; also, as with hypertonic saline, there was marked leakage of the ethanol back along the needle tract, with subsequent injury to surrounding tissue. Accordingly, we formulated ethanol into a gel (95% alcohol and an inactive polymer thickening agent). The gel injections were more contained within the renal tissue and produced less leakage along the needle tract. Ethanol gel alone produced lesions of reasonable size; however, these lesions contained skip areas of viable cells, thereby negating ethanol infusion alone as an effective ablative modality in the kidney. However, the lesion was twofold to threefold larger when ethanol was combined with monopolar or bipolar RF (50 W and 475 kHz for 5 minutes).

Acetic acid gel with or without monopolar and bipolar RF

Ohnishi and colleagues[138] reported that acetic acid had a stronger cytotoxic effect than pure ethanol in both animal studies and human studies of HCC. These investigators treated small (<3-cm) HCCs in 25 patients with multiple acetic acid injections with good therapeutic effect. The clinical results were followed with CT and fine-needle biopsy in all patients. Two patients eventually underwent partial hepatic resection. The 1-year survival rate among the 23 patients who did not undergo surgical treatment was 100%; the 2-year survival rate was 92%.

Mechanism of action: Acetic acid penetrates cells and can dissolve lipids and extract collagen.[138,139] Experiments with rats have shown that the necrotizing effect of acetic acid on liver cells is enhanced by increasing its concentration to a maximum of 50%; of note, its effect at a concentration of 15% was equal to that of absolute ethanol,[138] and at 50%, it was three times as effective than ethanol.[138] The use of the higher concentration of acetic acid (i.e., 50%) is preferable because it reduces the number of treatment sessions required.[140] A notable difference between acetic acid and ethanol is that the former, because of its low pH, appears to have good penetration into cancer cells in the tumor's capsule and into intratumoral septa; as a result, intratumoral fibers swell, and there is dissociation of intermolecular cross-links of collagen in the septa. Therefore, the number of treatment sessions may be fewer with acetic acid while the incidence of local recurrence is reduced.[141] Once injected into a tumor, acetic acid takes from several hours to a day to solubilize interstitial collagen (type I and III) and basement membrane collagen (type IV).

Renal ablation: Acetic acid has not been used previously for renal ablation. We first characterized and compared the volume, regularity, and histologic manifestations of renal lesions produced by the injection of 50% acetic acid immediately postoperatively and at 48 hours. Our initial results showed that acetic acid diffused into the tissues in an uncontrolled manner. It also leaked back along the needle tract and thus damaged surrounding tissues. Accordingly, we formulated a gel (50% acetic acid and an inactive polymer thickening agent). The injected gel remained more contained in the tissues. Acetic acid injections created an area of complete necrosis that was much larger than the volume injected; these lesions were also considerably larger than those created with hypertonic saline or ethanol. This observation would be compatible with the action of acetic acid, which is to dissolve cell membranes.

We further characterized whether RF with acetic acid could extend the zone of complete necrosis. Acetic acid gel with monopolar or bipolar RF (RF setting 50 W and 510 kHz for 5 minutes) resulted in lesions that were larger than those formed with acetic acid alone (20–21-mm *v* 14-mm length). There was complete necrosis within all lesions created with acetic acid plus RF.

CONCLUSIONS

The main aim of *in situ* needle ablation therapy is to use energy alone or combined with a noxious fluid to destroy an entire tumor without damaging adjacent vital structures. In this study, we looked at the majority of the available modalities for needle ablation: cryotherapy; microwave technology; RF, both dry and wet, using monopolar and bipolar needles; and chemoablation alone or combined with RF using hypertonic saline, ethanol, or acetic acid. With regard to the latter, we found that a unique gel formulation limited leakage of the chemoablative substance while maintaining the substances' noxious and conductive characteristics.

From our studies, it appears that with current technology, cryotherapy and multitine RF are the only modalities that offer complete necrosis within the sphere of treatment while allowing the surgeon to observe the delivery of the treatment ultrasonically. Microwave therapy, acetic acid injection, and monopolar or bipolar RF plus hypertonic saline or with acetic acid also create a lesion with complete necrosis; however, none of these lesions can at present be monitored accurately with real-time imaging. Of similar importance is that in our study, single-needle RF alone, both monopolar and bipolar, as well as ethanol or hypertonic saline alone produced lesions with incomplete necrosis (i.e., skip areas of viable cells).

In this new millennium, further improvements in needle ablative technology may ultimately lead to the routine outpatient treatment of most renal-cell cancers in the 1- to 4-cm range. Advances of this nature are completely in line with the concept that in a technologically advanced society, standard open surgical extirpation of most small cancers should no longer be necessary.

ACKNOWLEDGMENTS

We are grateful to the following persons for help with this study:

Ashvin Desai of Pro Surge/*Injectx*, 2195 Trade Zone Blvd., San Jose, CA 95131;

Eric Rudie of Urologix Incorporated, 14405 Twenty-First Ave. North, Minneapolis, MN 55447;

Joseph M. Caputo of Galil Medical USA, 400 West Cummings Park, Suite 4600, Woburn, MA 01801.

REFERENCES

1. Motzer RJ, Bander NH, Nanus DM. Renal-cell carcinoma [see comments]. N Engl J Med 1996;335:865.
2. Bosniak MA. Observation of small incidentally detected renal masses. Semin Urol Oncol 1995;13:267.
3. Homma Y, Kawabe K, Kitamura T, et al. Increased incidental detection and reduced mortality in renal cancer: Recent retrospective analysis at eight institutions. Int J Urol 1995;2:77.
4. Jayson M, Sanders H. Increased incidence of serendipitously discovered renal cell carcinoma. Urology 1998;51:203.
5. Dechet CB, Sebo T, Farrow G, et al. Prospective analysis of intraoperative frozen needle biopsy of solid renal masses in adults. J Urol 1999;162:1282.
6. Rodriguez R, Fishman EK, Marshall FF. Differential diagnosis and evaluation of the incidentally discovered renal mass. Semin Urol Oncol 1995;13:246.
7. Provet J, Tessler A, Brown J, et al. Partial nephrectomy for renal cell carcinoma: Indications, results and implications. J Urol 1991;145:472.
8. Walther MM, Choyke PL, Weiss G, et al. Parenchymal sparing surgery in patients with hereditary renal cell carcinoma. J Urol 1995;153:913.
9. Curry NS. Small renal masses (lesions smaller than 3 cm): Imaging evaluation and management. AJR Am J Roentgenol 1995; 164:355.
10. Herr HW. Partial nephrectomy for renal cell carcinoma with a normal opposite kidney. Cancer 1994;73:160.
11. Herr HW. Partial nephrectomy for unilateral renal carcinoma and a normal contralateral kidney: 10–year followup. J Urol 1999;161:33.
12. Sokoloff MH, deKernion JB, Figlin RA, et al. Current management of renal cell carcinoma. CA Cancer J Clin 1996;46:284.
13. Taylor RJ. Case for nephron-sparing surgery in managing renal cell carcinoma. Semin Urol 1993;11:104.
14. Licht MR, Novick AC. Nephron sparing surgery for renal cell carcinoma. J Urol 1993;149:1.
15. Lerner SE, Hawkins CA, Blute ML, et al. Disease outcome in patients with low stage renal cell carcinoma treated with nephron sparing or radical surgery. J Urol 1996;155:1868.
16. Walther MM, Choyke PL, Glenn G, et al. Renal cancer in families with hereditary renal cancer: Prospective analysis of a tumor size threshold for renal parenchymal sparing surgery. J Urol 1999;161:1475.
17. Fergany AF, Hafez KS, Novick AC. Long-term results of nephron sparing surgery for localized renal cell carcinoma: 10–year followup. J Urol 2000;163:442.
18. Nissenkorn I, Bernheim J. Multicentricity in renal cell carcinoma. J Urol 1995;153:620.
19. Hewitt PM, Zhao J, Akhter J, et al. A comparative laboratory study of liquid nitrogen and argon gas cryosurgery systems. Cryobiology 1997;35:303.
20. Gonder MJ, Soanes WA, Shulman S. Cryosurgical treatment of the prostate. Invest Urol 1966;3:372.
21. Bonney WW, Fallon B, Gerber WL, et al. Cryosurgery in prostatic cancer: Survival. Urology 1982;19:37.
22. Gage AA, Baust J. Mechanisms of tissue injury in cryosurgery. Cryobiology 1998;37:171.
23. Tatsutani K, Rubinsky B, Onik G, et al. Effect of thermal variables on frozen human primary prostatic adenocarcinoma cells. Urology 1996;48:441.
24. Mazur P. Cryobiology: The freezing of biological systems. Science 1970;168:939.
25. Rubinsky B, Lee CY, Bastacky J, et al. The process of freezing and the mechanism of damage during hepatic cryosurgery. Cryobiology 1990;27:85.
26. Neel HBD, Ketcham AS, Hammond WG. Requisites for successful cryogenic surgery of cancer. Arch Surg 1971;102:45.
27. Rubinsky B. The freezing process and mechanism of tissue damage. In: Onik G, Rubinsky B, Watson G, et al (eds): Percutaneous Prostate Cryoablation. St Louis: Quality Medical Publishing, 1995, chapter 4.
28. Chosy SG, Nakada SY, Lee FT Jr, et al. Monitoring renal cryosurgery: Predictors of tissue necrosis in swine. J Urol 1998;159:1370.
29. Gill E, Metamores E, Heffron T, et al. Laparoscopic renal cryoablation [abstract]. J Urol 1997;157:210A.
30. Campbell SC, Krishnamurthi V, Chow G, et al. Renal cryosurgery: Experimental evaluation of treatment parameters [see comments]. Urology 1998;52:29.
31. Gage AA. Cryosurgery in the treatment of cancer. Surg Gynecol Obstet 1992;174:73.
32. Baust J, Gage AA, Ma H, et al. Minimally invasive cryosurgery: Technological advances. Cryobiology 1997;34:373.
33. Gage AA, Augustynowicz S, Montes M, et al. Tissue impedance and temperature measurements in relation to necrosis in experimental cryosurgery. Cryobiology 1985;22:282.
34. Onik G, Rubinsky B, Zemel R, et al. Ultrasound-guided hepatic cryosurgery in the treatment of metastatic colon carcinoma: Preliminary results. Cancer 1991;67:901.
35. Lee FT Jr, Mahvi DM, Chosy SG, et al. Hepatic cryosurgery with intraoperative US guidance. Radiology 1997;202:624.
36. Lee F, Bahn DK, McHugh TA, et al. US-guided percutaneous cryoablation of prostate cancer. Radiology 1994;192:769
37. Savage SJ. Renal tumor ablation: Energy-based technologies. World J Urol 1000;18:283.
38. Bishoff JT, Chen RB, Lee BR, et al. Laparoscopic renal cryoablation: Acute and long-term clinical, radiographic, and pathologic effects in an animal model and application in a clinical trial. J Endourol 1999;13:233.
39. Nakada SY, Lee FT Jr, Warner T, et al. Laparoscopic cryosurgery of the kidney in the porcine model: An acute histological study. Urology 1998;51:161.
40. Stephenson RA, King DK, Rohr LR. Renal cryoablation in a canine model. Urology 1996;47:772.
41. Cozzi PJ, Lynch WJ, Collins S, et al. Renal cryotherapy in a sheep model: A feasibility study. J Urol 1997;157:710.
42. Sindelar WF, Javadpour N, Bagley DH. Histological and ultrastructural changes in rat kidney after cryosurgery. J Surg Oncol 1981;18:363.
43. Nakada SY, Lee FT Jr, Warner TF, et al. Laparoscopic renal cryotherapy in swine: Comparison of puncture cryotherapy preceded by arterial embolization and contact cryotherapy. J Endourol 1998;12:567.
44. McMasters KM, Edwards MJ. Liver cryosurgery. J Ky Med Assoc 1996;94:222.
45. Lee FT Jr, Chosy SG, Littrup PJ, et al. CT-monitored percutaneous cryoablation in a pig liver model: Pilot study. Radiology 1999;211:687.
46. Sandison GA, Loye MP, Rewcastle JC, et al. X-ray CT monitoring of iceball growth and thermal distribution during cryosurgery. Phys Med Biol 1998;43:3309.
47. Matsumoto R, Oshio K, Jolesz FA. Monitoring of laser and freezing-induced ablation in the liver with T1-weighted MR imaging. J Magn Reson Imaging 1992;2:555.

48. Matsumoto R, Selig AM, Colucci VM, et al. MR monitoring during cryotherapy in the liver: Predictability of histologic outcome. J Magn Reson Imaging 1993;3:770.
49. Pease GR, Wong ST, Roos MS, et al. MR image-guided control of cryosurgery. J Magn Reson Imaging 1995;5:753.
50. Hong JS, Wong S, Pease G, et al. MR imaging assisted temperature calculations during cryosurgery. Magn Reson Imaging 1994;12:1021.
51. Tacke J, Adam G, Speetzen R, et al. MR-guided interstitial cryotherapy of the liver with a novel, nitrogen-cooled cryoprobe. Magn Reson Med 1998;39:354.
52. Remer EM, Hale JC, O'Malley CM, et al. Sonographic guidance of laparoscopic renal cryoablation. AJR Am J Roentgenol 2000;174:1595.
53. Goldberg SN, Gazelle GS, Mueller PR. Thermal ablation therapy for focal malignancy: A unified approach to underlying principles, techniques, and diagnostic imaging guidance [see comments]. AJR Am J Roentgenol 2000;174:323.
54. Uchida M, Imaide Y, Sugimoto K, et al. Percutaneous cryosurgery for renal tumours. Br J Urol 1995;75:132.
55. Shingleton WB, Sewell PE Jr. Percutaneous renal tumor cryoablation with magnetic resonance imaging guidance. J Urol 2001; 165:773.
56. Gill IS, Novick AC, Soble JJ, et al. Laparoscopic renal cryoablation: Initial clinical series. Urology 1998;52:543.
57. Zegel HG, Holland GA, Jennings SB, et al. Intraoperative ultrasonographically guided cryoablation of renal masses: Initial experience. J Ultrasound Med 1998;17:571.
58. Weber SM, Lee FT Jr, Warner TF, et al. Hepatic cryoablation: US monitoring of extent of necrosis in normal pig liver. Radiology 1998;207:73.
59. Schuder G, Pistorius G, Schneider G, et al. Preliminary experience with percutaneous cryotherapy of liver tumours. Br J Surg 1998;85:1210.
60. Adam R, Majno P, Castaing D, et al. Treatment of irresectable liver tumours by percutaneous cryosurgery. Br J Surg 1998;85: 1493.
61. Rosette JJ de la, D'Ancona FC, Debruyne FM. Current status of thermotherapy of the prostate. J Urol 1997;157:430.
62. Francisca EA, Kortmann BB, Floratos DL, et al. Tolerability of 3.5 versus 2.5 high-energy transurethral microwave thermotherapy. Eur Urol 2000;38:59.
63. Kigure T, Harada T, Yuri Y, et al. Ultrasound-guided microwave thermotherapy on a VX-2 carcinoma implanted in rabbit kidney. Ultrasound Med Biol 1995;21:649.
64. Muraki J, Cord J, Addonizio JC, et al. Application of microwave tissue coagulation in partial nephrectomy. Urology 1991;37:282.
65. Naito S, Nakashima M, Kimoto Y, et al. Application of microwave tissue coagulator in partial nephrectomy for renal cell carcinoma. J Urol 1998;159:960.
66. Kagebayashi Y, Hirao Y, Samma S, et al. In situ non-ischemic enucleation of multilocular cystic renal cell carcinoma using a microwave coagulator. Int J Urol 1995;2:339.
67. Kigure T, Harada T, Yuri Y, et al. Laparoscopic microwave thermotherapy on small renal tumors: Experimental studies using implanted VX-2 tumors in rabbits. Eur Urol 1996;30:377.
68. Devonec M, Tomera K, Perrin P. Review: Transurethral microwave thermotherapy in benign prostatic hyperplasia. J Endourol 1993;7:255.
69. Devonec M, Berger N, Fendler JP, et al. Thermoregulation during transurethral microwave thermotherapy: Experimental and clinical fundamentals. Eur Urol 1993;23:63.
70. Djavan B, Shariat S, Schafer B, et al. Tolerability of high energy transurethral microwave thermotherapy with topical urethral anesthesia: Results of a prospective, randomized, single-blinded clinical trial [see comments]. J Urol 1998;160:772.
71. Djavan B, Roehrborn CG, Shariat S, et al. Prospective randomized comparison of high energy transurethral microwave thermotherapy versus alpha-blocker treatment of patients with benign prostatic hyperplasia. J Urol 1999;161:139.
72. Larson TR, Blute ML, Tri JL, et al. Contrasting heating patterns and efficiency of the Prostatron and Targis microwave antennae for thermal treatment of benign prostatic hyperplasia. Urology 1998;51:908.
73. Djavan B, Larson TR, Blute ML, et al. Transurethral microwave thermotherapy: What role should it play versus medical management in the treatment of benign prostatic hyperplasia? Urology 1998;52:935.
74. Seegenschmiedt MH, Brady LW, Sauer R. Interstitial thermoradiotherapy: Review of technical and clinical aspects. Am J Clin Oncol 1990;13:352.
75. Overgaard J. Hyperthermia as an adjuvant to radiotherapy: Review of the randomized multicenter studies of the European Society for Hyperthermic Oncology. Strahlenther Onkol 1987; 163:453.
76. Larson TR, Bostwick DG, Corica A. Temperature-correlated histopathologic changes following microwave thermoablation of obstructive tissue in patients with benign prostatic hyperplasia. Urology 1996;47:463.
77. Goldberg SN, Gazelle GS, Halpern EF, et al. Radiofrequency tissue ablation: Importance of local temperature along the electrode tip exposure in determining lesion shape and size. Acad Radiol 1996;3:212.
78. Thomsen S. Pathologic analysis of photothermal and photomechanical effects of laser–tissue interactions. Photochem Photobiol 1991;53:825.
79. Goldberg SN, Hahn PF, Tanabe KK, et al. Percutaneous radiofrequency tissue ablation: Does perfusion-mediated tissue cooling limit coagulation necrosis? J Vasc Interv Radiol 1998; 9:101.
80. Goldberg SN, Hahn PF, Halpern EF, et al. Radio-frequency tissue ablation: Effect of pharmacologic modulation of blood flow on coagulation diameter. Radiology 1998;209:761.
81. Patterson EJ, Scudamore CH, Owen DA, et al. Radiofrequency ablation of porcine liver in vivo: Effects of blood flow and treatment time on lesion size. Ann Surg 1998;227:559.
82. Heisterkamp J, Hillegersberg R van, Mulder PG, et al. Importance of eliminating portal flow to produce large intrahepatic lesions with interstitial laser coagulation. Br J Surg 1997;84:1245.
83. Eliasson T, Damber JE. Temperature controlled high energy transurethral microwave thermotherapy for benign prostatic hyperplasia using a heat shock strategy [see comments]. J Urol 1998;160:777.
84. Mauroy B, Chive M, Stefaniak X, et al. Study of the effects of thermotherapy in benign prostatic hypertrophy. Eur Urol 1997; 32:198.
85. Bolmsjo M, Wagrell L, Hallin A, et al. The heat is on—But how? A comparison of TUMT devices. Br J Urol 1996;78:564.
86. Blute ML, Larson TR, Hanson KA, et al. Current status of transurethral thermotherapy at the Mayo Clinic. Mayo Clin Proc 1998;73:597.
87. Clark W. Oscillatory desiccation in the treatment malignant growths and minor surgical conditions. J Adv Ther 1911;29:169.
88. Cushing H. Electrosurgery as an aid to the removal of intracranial tumors. Surg Gynecol Obstet 1928;47:751.
89. Livraghi T, Goldberg SN, Monti F, et al. Saline-enhanced radiofrequency tissue ablation in the treatment of liver metastases. Radiology 1997;202:205.
90. Rossi S, Di Stasi M, Buscarini E, et al. Percutaneous radiofrequency interstitial thermal ablation in the treatment of small hepatocellular carcinoma. Cancer J Sci Am 1995;1:73.
91. Solbiati L, Ierace T, Goldberg SN, et al. Percutaneous US-guided

radio-frequency tissue ablation of liver metastases: Treatment and follow-up in 16 patients. Radiology 1997;202:195.
92. McGahan JP, Nyberg DA, Mack LA. Sonography of facial features of alobar and semilobar holoprosencephaly. AJR Am J Roentgenol 1990;154:143.
93. Organ LW. Electrophysiologic principles of radiofrequency lesion making. Appl Neurophysiol 1976;39:69.
94. Wittkampf FH, Hauer RN, Robles de Medina EO. Control of radiofrequency lesion size by power regulation. Circulation 1989; 80:962.
95. Seki T, Wakabayashi M, Nakagawa T, et al. Ultrasonically guided percutaneous microwave coagulation therapy for small hepatocellular carcinoma. Cancer 1994;74:817.
96. Cline HE, Hynynen K, Watkins RD, et al. Focused US system for MR imaging-guided tumor ablation. Radiology 1995;194:731.
97. Siperstein AE, Rogers SJ, Hansen PD, et al. Laparoscopic thermal ablation of hepatic neuroendocrine tumor metastases. Surgery 1997;122:1147.
98. Goldberg SN, Gazelle GS, Dawson SL, et al. Tissue ablation with radiofrequency using multiprobe arrays. Acad Radiol 1995;2:670.
99. Merkle EM, Goldberg SN, Boll DT, et al. Effects of superparamagnetic iron oxide on radio-frequency-induced temperature distribution: In vitro measurements in polyacrylamide phantoms and in vivo results in a rabbit liver model. Radiology 1999;212:459.
100. Djavan B, Zlotta AR, Susani M, et al. Transperineal radiofrequency interstitial tumor ablation of the prostate: Correlation of magnetic resonance imaging with histopathologic examination. Urology 1997;50:986.
101. Djavan B, Susani M, Shariat S, et al. Transperineal radiofrequency interstitial tumor ablation (RITA) of the prostate. Techn Urol 1998;4:103.
102. Djavan B, Partin AW, Hoey MF, et al. Transurethral radiofrequency therapy for benign prostatic hyperplasia using a novel saline-liquid conductor: The virtual electrode. Urology 2000;55:13.
103. Hoey MF, Mulier PM, Leveillee RJ, et al. Transurethral prostate ablation with saline electrode allows controlled production of larger lesions than conventional methods. J Endourol 1997; 11:279.
104. Leveillee RJ, Hoey MF, Hulbert JC, et al. Enhanced radiofrequency ablation of canine prostate utilizing a liquid conductor: The virtual electrode. J Endourol 1996;10:5.
105. Hoey MF, Dixon CM, Paul S. Transurethral prostate ablation using saline-liquid electrode introduced via flexible cystoscope. J Endourol 1998;12:461.
106. Patel VR, Leveillee RJ, Hoey MF, et al. Radiofrequency ablation of rabbit kidney using liquid electrode: Acute and chronic observations. J Endourol 2000;14:155.
107. McGahan JP, Browning PD, Brock JM, et al. Hepatic ablation using radiofrequency electrocautery. Invest Radiol 1990;25:267.
108. Zlotta AR, Raviv G, Peny MO, et al. [A new method of cancer treatment: The use of radiofrequencies in urological tumors]. Acta Urol Belg 1996;64:1.
109. Zlotta AR, Wildschutz T, Raviv G, et al. Radiofrequency interstitial tumor ablation (RITA) is a possible new modality for treatment of renal cancer: *Ex vivo* and *in vivo* experience. J Endourol 1997;11:251.
110. McGovern FJ, Wood BJ, Goldberg SN, et al. Radio frequency ablation of renal cell carcinoma via image guided needle electrodes. J Urol 1999;161:599.
111. Sullman A, Resnick M, Oefelein M, et al. MRI-guided radiofrequency interstitial thermal ablation of renal tumors: A minimally invasive alternative to traditional surgical approaches. J Urol 2000;163:7.
112. Pavlovich C, Wood B, Choyke P, et al. Radiofrequency interstitial thermal ablation (RITA) of small renal tumors in Von Hippel-Lindau disease. J Urol 2000;163:8.
113. Walther MC, Shawker TH, Libutti SK, et al. A Phase 2 study of radio frequency interstitial tissue ablation of localized renal tumors. J Urol 2000;163:1424.
114. Michaels MJ, Silverman M, Libertino JA. Absence of total tumor necrosis in radiofrequency ablated renal tumors [abstract 89]. J Urol 2001;165(suppl):21.
115. Rendon R, Gertner M, Kachura J, et al. Radiofrequency ablation techniques for renal cell carcinoma (RCC) require further development [abstract 90]. J Urol 2001;165(suppl):21.
116. Sweet J, Rendon R, Gertner M, et al. Morphologic assessment of radiofrequency (RF) therapy for renal cell carcinoma (RCC) reveals incomplete renal ablation [abstract 91]. J Urol 2001;165(suppl):21.
117. Rendon RA, Kachura JR, Sweet JM, et al. The uncertainty of radio frequency treatment of renal cell carcinoma: Findings at immediate and delayed nephrectomy. J Urol 2002;167:1587.
118. Gervais DA, McGovern FJ, Arellano RS, et al. Renal cell carcinoma: Clinical experience and technical success with radio-frequency ablation of 42 tumors. Radiology 2002;226:417.
119. de Baere T, Kuoch V, Smayra T, et al. Radio frequency ablation of renal cell carcinoma: Preliminary clinical experience. J Urol 2002;167:1961.
120. Honda N, Guo Q, Uchida H, et al. Percutaneous hot saline injection therapy for hepatic tumors: An alternative to percutaneous ethanol injection therapy. Radiology 1994;190:53.
121. el Mouaasouy A, Naruhn M, Lauchart W, et al. [Treatment of symptomatic non-parasitic liver cysts using percutaneous drainage and irrigation with hypertonic saline solution]. Chirurg 1991;62:810.
122. McCoy S, Evans A, Spurrier N. Sclerotherapy for leg telangiectasia: A blinded comparative trial of polidocanol and hypertonic saline. Dermatol Surg 1999;25:381.
123. Goldman MP, Weiss RA, Brody HJ, et al: Treatment of facial telangiectasia with sclerotherapy, laser surgery, and/or electrodesiccation: a review. J Dermatol Surg Oncol, 1993;19:899.
124. Sadick NS. Sclerotherapy of varicose and telangiectatic leg veins: Minimal sclerosant concentration of hypertonic saline and its relationship to vessel diameter. J Dermatol Surg Oncol 1991;17:65.
125. Weiss RA, Weiss MA. Incidence of side effects in the treatment of telangiectasias by compression sclerotherapy: Hypertonic saline vs. polidocanol. J Dermatol Surg Oncol 1990;16:800.
126. Goldman MP, Bennett RG. Treatment of telangiectasia: A review. J Am Acad Dermatol 1987;17:167.
127. Ellman BA, Parkhill BJ, Curry TS, et al. Ablation of renal tumors with absolute ethanol: A new technique. Radiology 1981;141:619.
128. Lee W, Kim TS, Chung JW, et al. Renal angiomyolipoma: Embolotherapy with a mixture of alcohol and iodized oil. J Vasc Interv Radiol 1998;9:255.
129. Jitsukawa S, Tachibana M, Deguchi N, et al. Renal devitalization with ethanol injection in management of patients with advanced hypernephroma. Urology 1984;23:87.
130. Sugiura N, Takara K, Ohto M, et al. Treatment of small hepatocellular carcinoma by percutaneous injection of ethanol into tumour with real time ultrasound monitoring. Acta Hepatol Jpn 1983;24:920.
131. Uflacker R, Paolini RM, Nobrega M. Ablation of tumor and inflammatory tissue with absolute ethanol. Acta Radiol [Diagn] (Stockh) 1986;27:131.
132. Burgener FA, Steinmetz SD. Treatment of experimental adenocarcinomas by percutaneous intratumoral injection of absolute ethanol. Invest Radiol 1987;22:472.
133. Fujimoto T. The experimental and clinical studies of percutaneous ethanol injection therapy (PEIT) under ultrasonography for small hepatocellular carcinoma. Acta Hepatol Jpn 1988;29:52.
134. Kawano M. An experimental study of percutaneous absolute ethanol injection therapy for small hepatocellular carcinoma: Effects of absolute ethanol on the healthy canine liver. Gastroenterol Jpn 1989;24:663.

135. Festi D, Monti F, Casanova S, et al. Morphological and biochemical effects of intrahepatic alcohol injection in the rabbit. J Gastroenterol Hepatol 1990;5:402.
136. Shiina S, Tagawa K, Unuma T, et al. Percutaneous ethanol injection therapy for hepatocellular carcinoma: A histopathologic study. Cancer 1991;68:1524.
137. Ebara M, Kita K, Nagato Y, et al. [Percutaneous ethanol injection (PEI) for small hepatocellular carcinoma]. Gan To Kagaku Ryoho 1993;20:884.
138. Ohnishi K, Ohyama N, Ito S, et al. Small hepatocellular carcinoma: Treatment with US-guided intratumoral injection of acetic acid. Radiology 1994;193:747.
139. Miller EJ, Rhodes RK. Preparation and characterization of the different types of collagen. Methods Enzymol 1982;82:33.
140. Ohnishi K, Nomura F, Ito S, et al. Prognosis of small hepatocellular carcinoma (less than 3 cm) after percutaneous acetic acid injection: Study of 91 cases. Hepatology 1996;23:994.
141. Ohnishi K, Yoshioka H, Ito S, et al. Treatment of nodular hepatocellular carcinoma larger than 3 cm with ultrasound-guided percutaneous acetic acid injection. Hepatology 1996;24:1379.
142. Bush IM, Santoni E, Lieberman PH, et al. Some effects of freezing the rat kidney in situ. Cryobiology 1964;1:163.
143. Breining H, Helpap B, Minderjahn A, et al. Histological and autoradiographic findings in cryonecrosis of the liver and kidney. Cryobiology 1974;11:519.
144. Helpap B, Grouls V, Lange O, et al. Morphologic and cell kinetic investigations of the spleen after repeated in situ freezing of liver and kidney. Pathol Res Pract 1979;164:167.
145. Barone GW, Rodgers BM. Morphologic and functional effects of renal cryoinjury. Cryobiology 1988;25:363.
146. Onik GM, Reyes G, Cohen JK, et al. Ultrasound characteristics of renal cryosurgery. Urology 1993;42:212.
147. Sung GT, Gill IS, Hsu H, et al. Effect of intentional cryoinjury to the renal collecting system [abstract]. J Endourol 1999;13(suppl): A13.
148. Chen RN, Bishoff JT, Jackman S, et al. Doppler US and CT evaluation the kidney the kidney following cryosurgical ablation in a porcine model [abstract]. J Endourol 1999;13(suppl):A13.
149. Nakada SY, Jerde T, Lee FJ, et al. Efficacy of cryotherapy and nephrectomy in treating implanted VX-2 carcinoma in rabbit kidney [abstract]. J Endourol 1999;13(suppl):A13.
150. Delworth MG, Pisters LL, Fornage BD, et al. Cryotherapy for renal cell carcinoma and angiomyolipoma. J Urol 1996;155:252.
151. McGinnins D, Strup S. Laparoscopic cryosurgery of renal tumors: A promising new technique [abstract]. J Endourol 1998;12(suppl): S153.
152. Orihuela E, vanSonnenberg E, Motamedi M, et al. Effect of warm arterial blood flow and multiple cryotherapy probes on cryotherapy of renal cell carcinoma (RCC) [abstract]. J Endourol 1999;13(suppl):A13.
153. Gill IS, Novick AC, Meraney AM, et al. Laparoscopic renal cryoablation in 32 patients. Urology 2000;56:748.
154. Steinberg A, Strzempkowsk IB, Kaouk JH, et al. 3–year and greater follow-up of laparoscopic renal cryoablation [abstract]. J Endourol 2002;16(suppl):A-150.
155. Shingleton WB. Long term result of percutaneous cryoablation [abstract 8]. J Urol 2003;169(suppl):2.
156. Kigure T, Harada T, Yuri Y, et al. Experimental study of microwave coagulation of a VX-2 carcinoma implanted in rabbit kidney. Int J Urol 1994;1:23.
157. Itoh K, Suzuki Y, Miuru M, et al. Posterior retroperitoneoscopic partial nephrectomy using microwave tissue coagulator for small renal tumors. J Endourol 2002;16:367.
158. Murota T, Kawakita M, Oguchi N, et al. Retroperitoneoscopic partial nephrectomy using microwave coagulation for small renal tumors. Eur Urol 2002;41:540.
159. Polascik TJ, Hamper U, Lee BR, et al. Ablation of renal tumors in a rabbit model with interstitial saline-augmented radiofrequency energy: Preliminary report of a new technology [see comments]. Urology 1999;53:465.
160. Merkle EM, Shonk JR, Duerk JL, et al. MR-guided RF thermal ablation of the kidney in a porcine model. AJR Am J Roentgenol 1999;173:645.
161. Jerde T, Johnson C, Lee FJ, et al. Efficacy of therapeutic techniques for implanted VX2 carcinoma in rabbit kidneys: Comparison between radiofrequency, cryoablation and nephrectomy. J Urol 2000;163:8.
162. Gill IS, Hsu TH, Fox RL, et al. Laparoscopic and percutaneous radiofrequency ablation of the kidney: Acute and chronic porcine study. Urology 2000;56:197.
163. Hsu TH, Fidler ME, Gill IS. Radiofrequency ablation of the kidney: Acute and chronic histology in porcine model. Urology 2000;56:872.
164. Hall WH, McGahan JP, Link DP, et al. Combined embolization and percutaneous radiofrequency ablation of a solid renal tumor. AJR Am J Roentgenol 2000;174:1592.
165. Gervais DA, McGovern FJ, Wood BJ, et al. Radio-frequency ablation of renal cell carcinoma: Early clinical experience. Radiology 2000;217:665.
166. Pavlovich CP, Walther MM, Choyke PL, et al. Percutaneous radio frequency ablation of small renal tumors: Initial results. J Urol 2002;167:10.
167. Matlaga BR, Zagoria RJ, Woodruff RD, et al. Phase II trial of radio frequency ablation of renal cancer: Evaluation of the kill zone. J Urol 2002;168:2401.
168. Michaels MJ, Rhee HK, Mourtzinos AP, et al. Incomplete renal tumor destruction using radio frequency interstitial ablation. J Urol 2002;168:2406.

Address reprint requests to:
Ralph V. Clayman, M.D.
Dept. of Urology
UCI Medical Center
101 City Drive, Building 55 Room 304
Route 81, Orange, CA 92868

E-mail: rclayman@uci.edu